Electronic Supplementary Material (ESI) for Dalton Transactions.

The irregular synthesis of the iron(III) terephthalate metal-organic frameworks MOF-235 and MIL-101

Isabelle Simonsson[1], Philip Gärdhagen[1], Moira Andrén[1], Pui Lam Tam[2], Zareen Abbas[1]

[1]Department of Chemistry and Molecular Biology, University of Gothenburg, Gothenburg, Sweden

[2]Industrial and Materials Science, Chalmers University of Technology, Gothenburg, Sweden

Supplementary information

Figures.

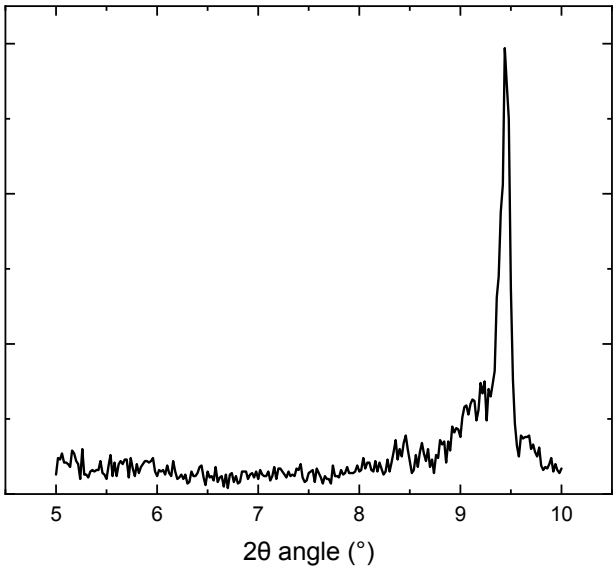

Figure S1: P-XRD of the product of the conventional MOF-235 synthesis protocol (1:1 DMF:ethanol, 3:5 Fe(III):TPA), with the exception of using a synthesis temperature of 70°C.

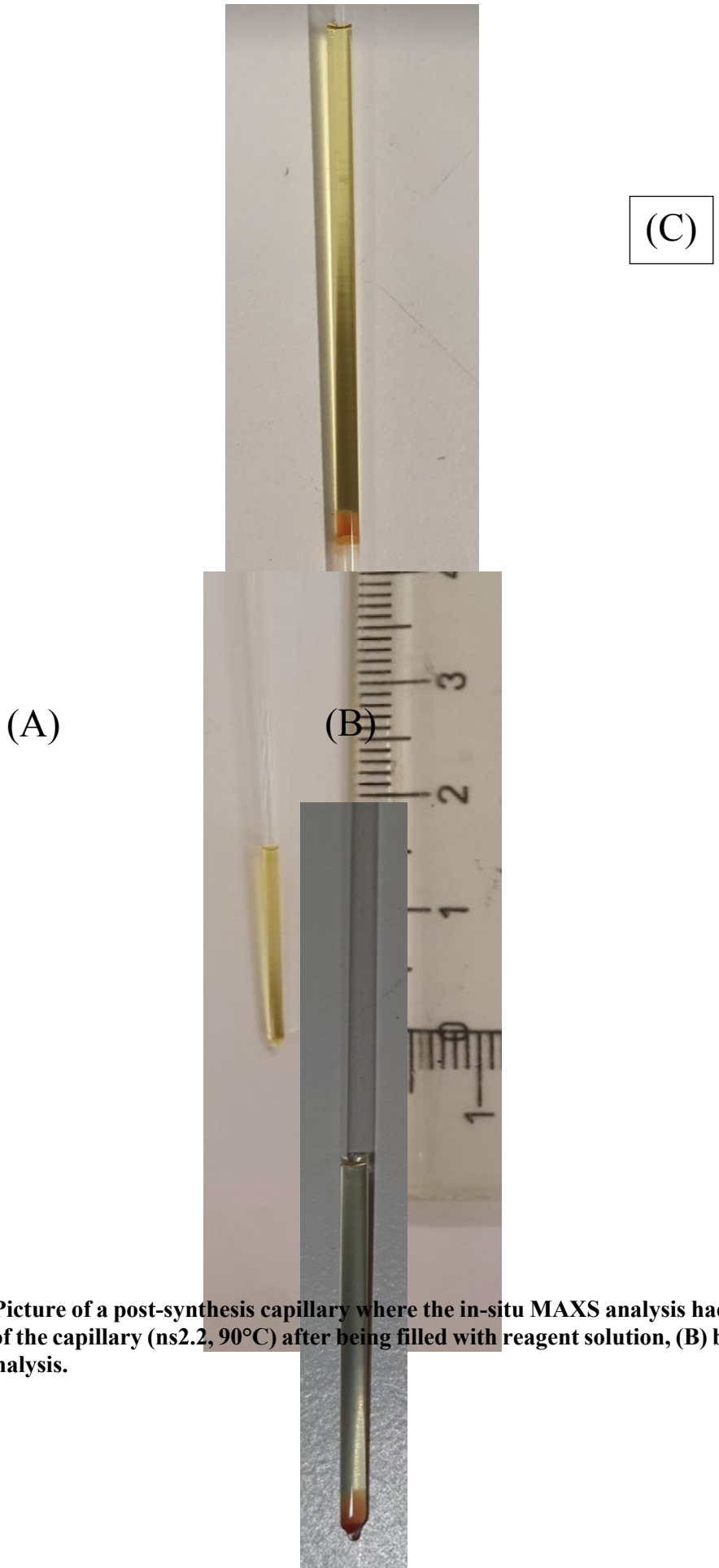

Figure S2: (A) Picture of a post-synthesis capillary where the in-situ MAXS analysis had failed (ns2.5, 80°C). Picture of the capillary (ns2.2, 90°C) after being filled with reagent solution, (B) before analysis and (C) after analysis.

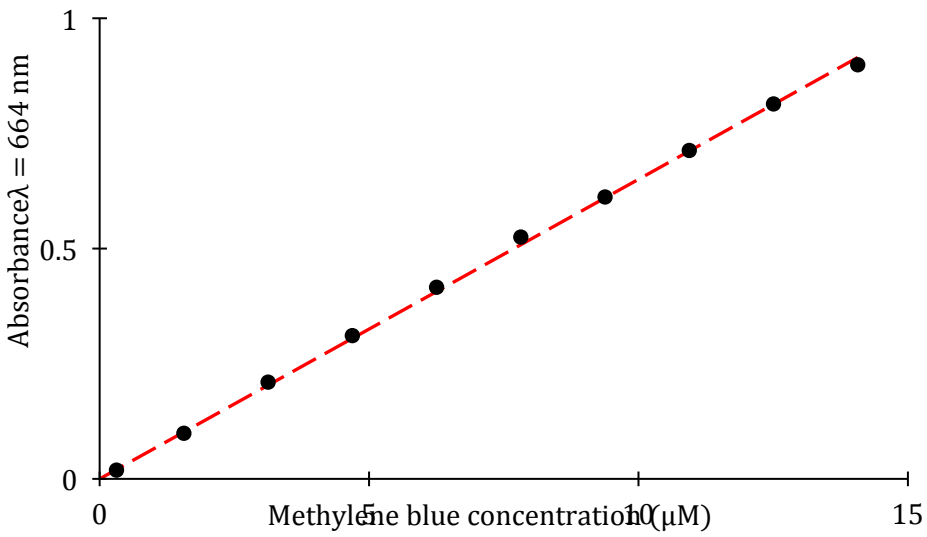

Figure S3: Calibration curve of methylene blue in the concentration range 0.313 µM (0.1 ppm) to 14.1 µM (4.5 ppm).

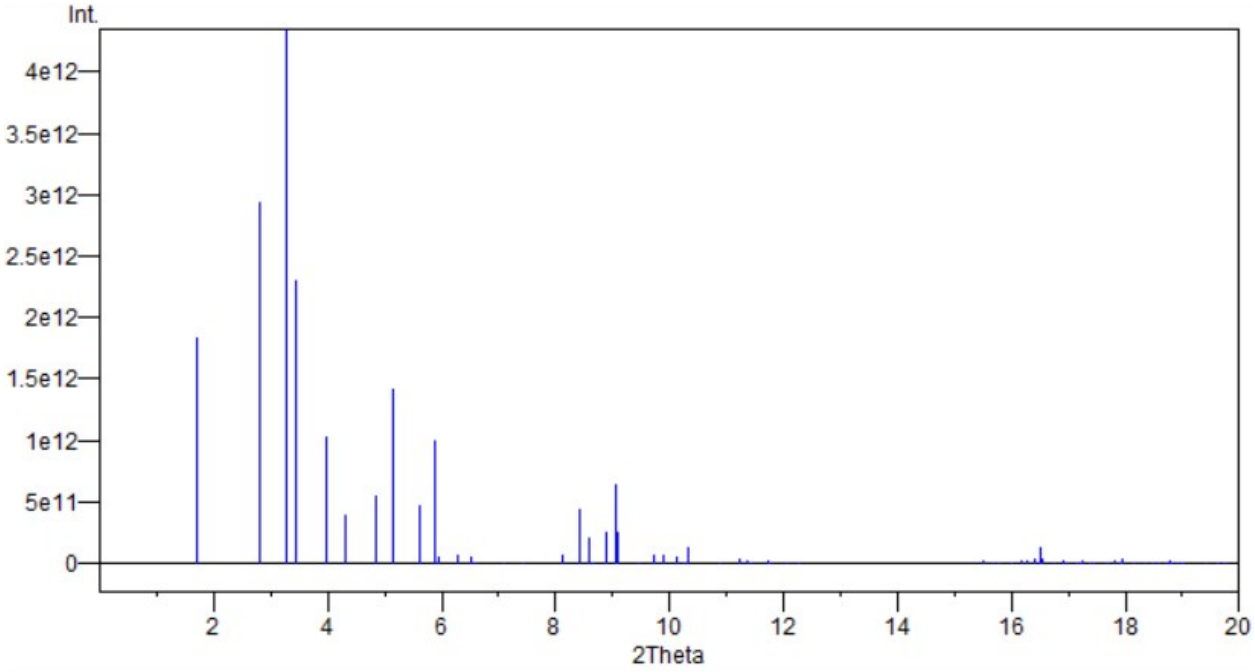

Figure S4: Reference diffractogram (λ = 1.54 Å) of Cr-MIL-101 created in the Diamond software[1] from a cif file published by Lebedev et al., 2005 [2].

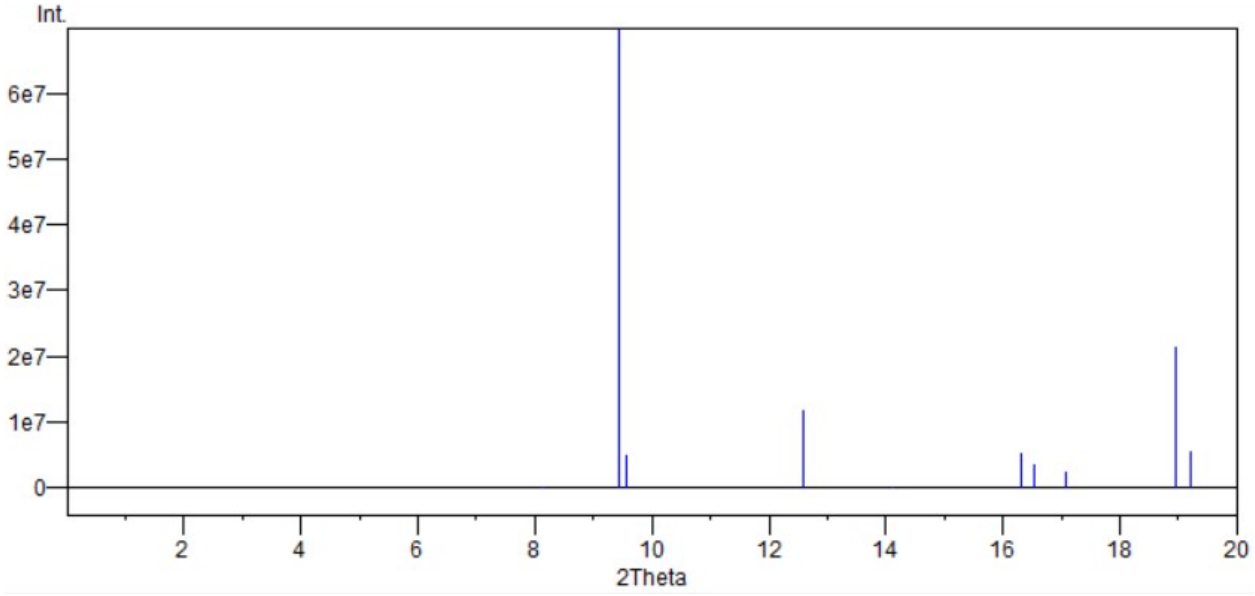

Figure S5: Reference diffractogram (λ = 1.54 Å) of Fe-MOF-235 created in the Diamond software from a cif file published by Sudik et al., 2005 [3].

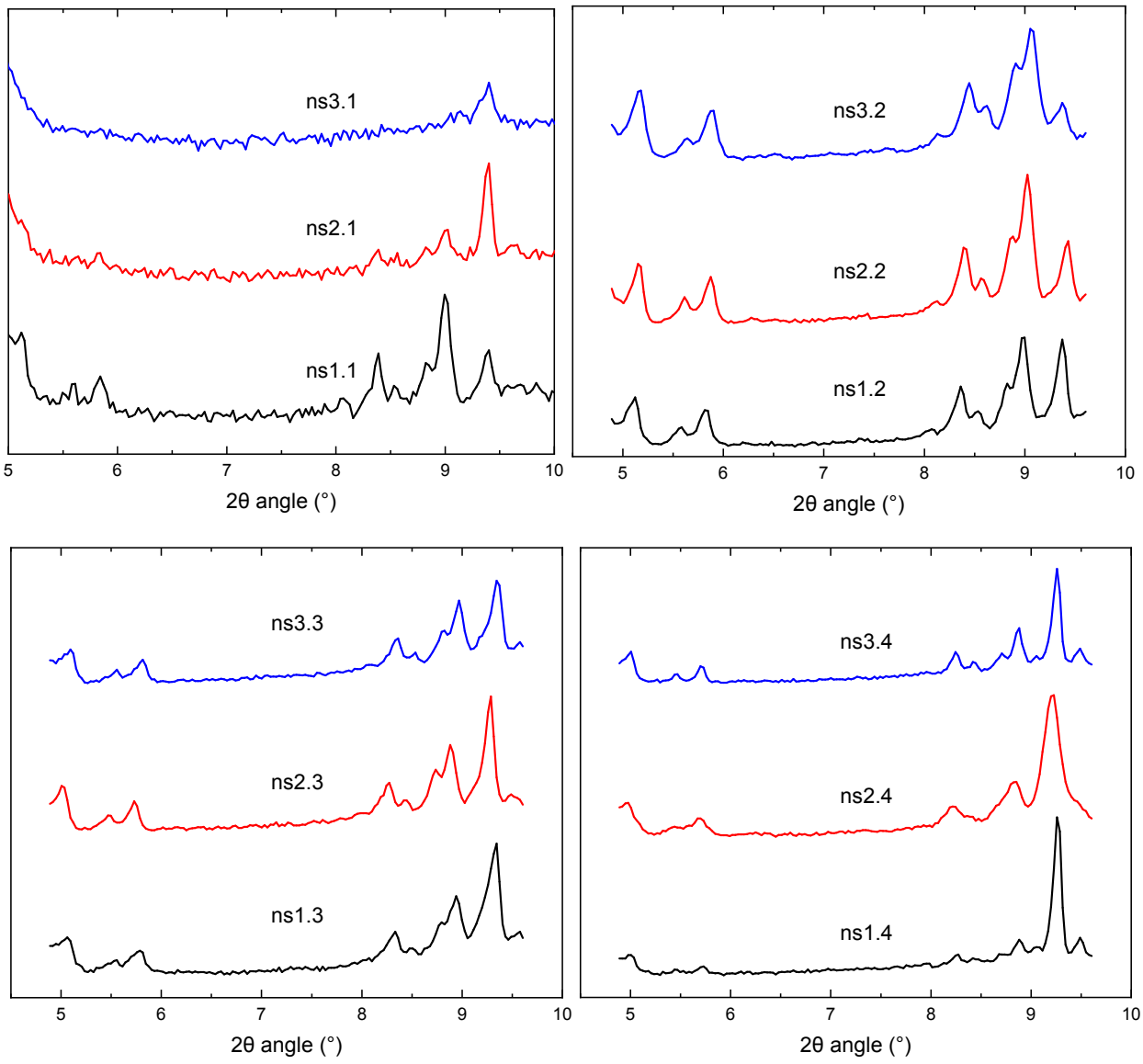

Figure S6: P-XRD (Cu Kα radiation source) patterns in the 5-10° range of the nsX.1-4 synthesis products.

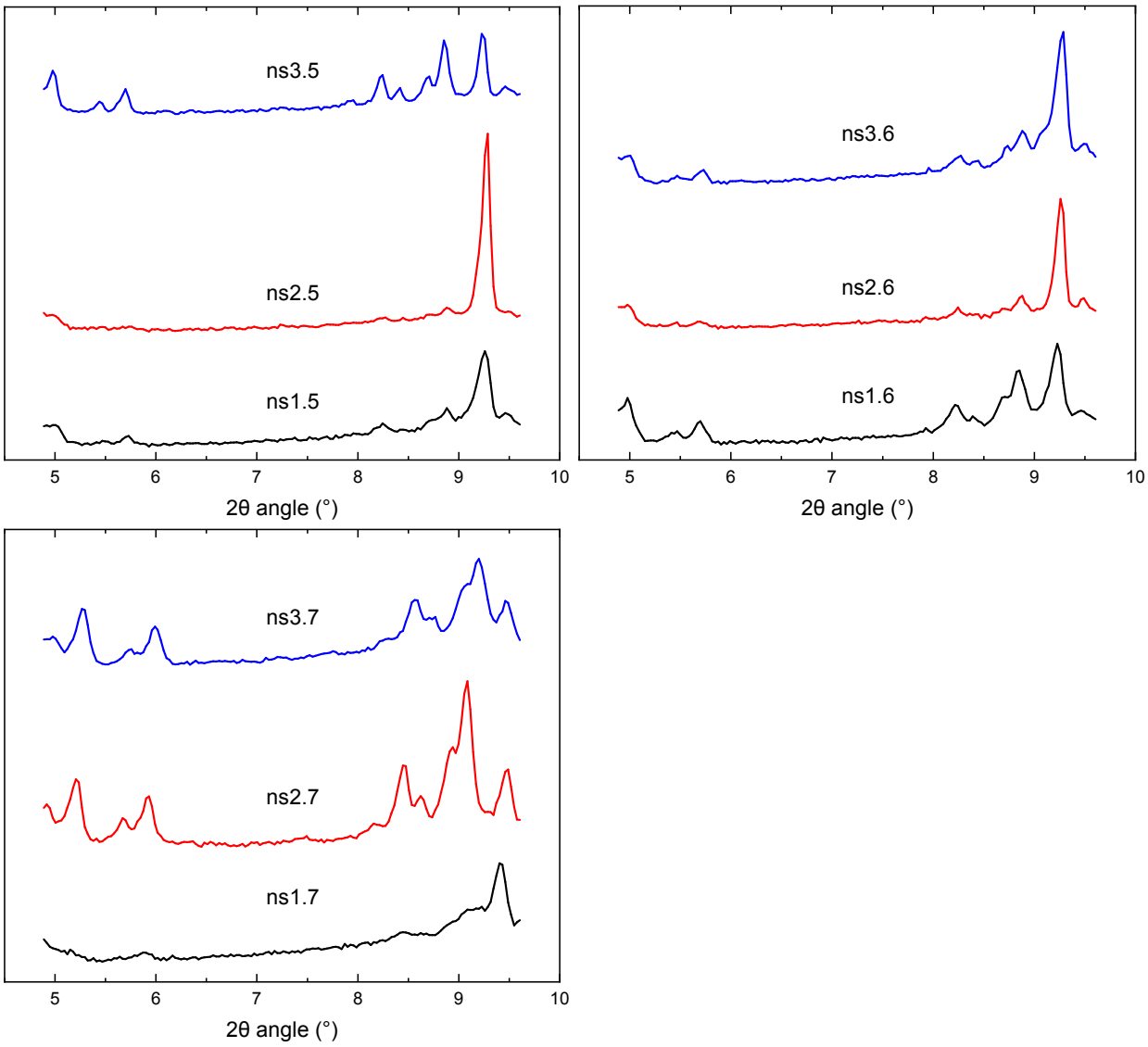

Figure S7: P-XRD (Cu Kα radiation source) patterns in the 5-10° range of the nsX.5-7 synthesis products.

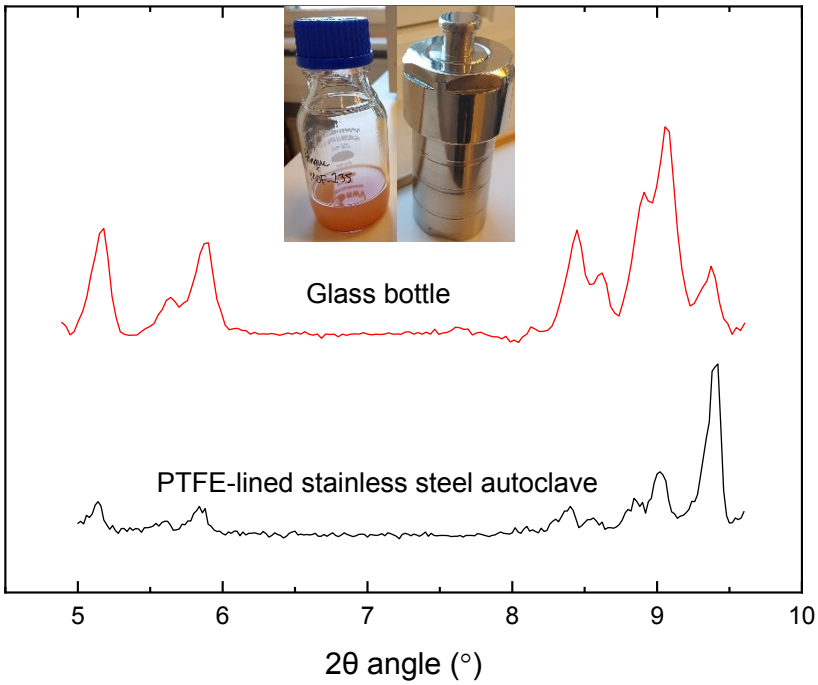

Figure S8: Comparison of the P-XRD patterns of the ns3.2 synthesis in two different reaction vessels. The inset shows the respective containers.

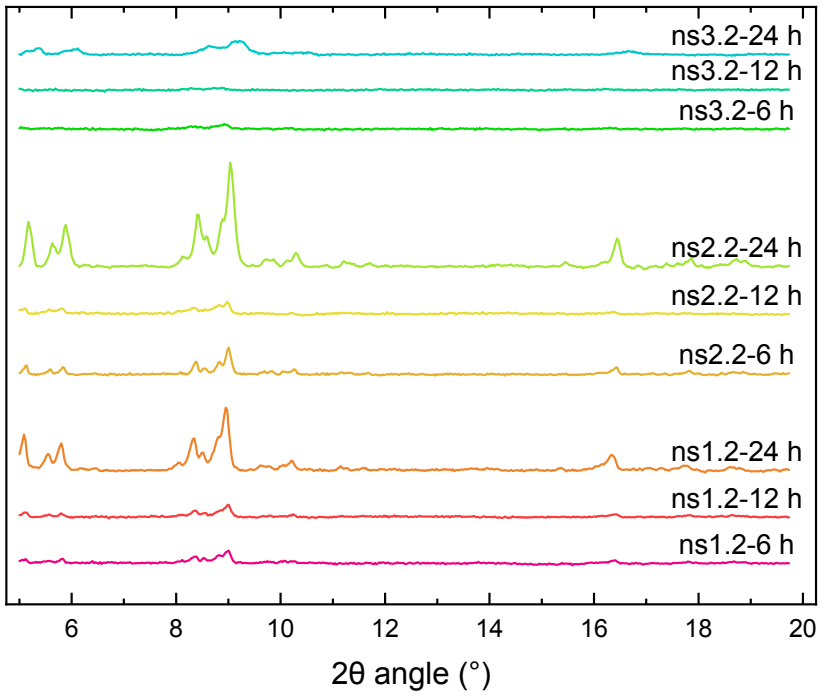

Product	BET surface area (m^2/g)
ns3.2-24 h	**1871**
ns3.2-12 h	**457**
ns3.2-6 h	**622**
ns2.2-24 h	**3280**
ns2.2-12 h	**2023**
ns2.2-6 h	**1641**
ns1.2-24 h	**3293**
ns1.2-12 h	**595**
ns1.2-6 h	**1143**

Figure S9: XRD diffractograms of the ex-situ synthesis products with 1:1 DMF:etOH ratio at times 6, 12, 24 h. The table to the right shows the determined BET surface areas of the same products.

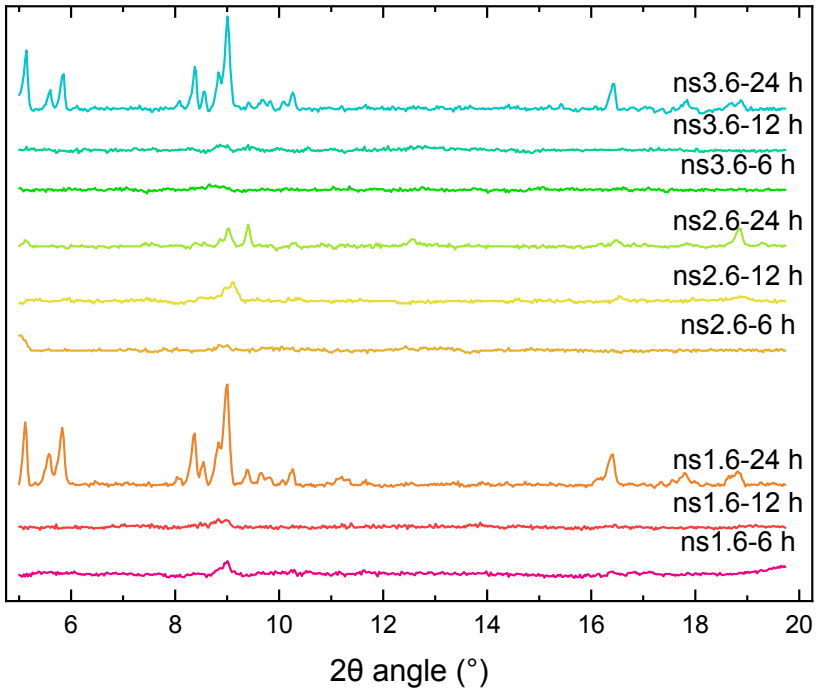

Product	BET surface area (m^2/g)
ns3.6-24 h	**510**
ns3.6-12 h	**507**
ns3.6-6 h	**1105**
ns2.6-24 h	**305**
ns2.6-12 h	**462**
ns2.6-6 h	**387**
ns1.6-24 h	**444**
ns1.6-12 h	**493**
ns1.6-6 h	**405**

Figure S10: XRD diffractograms of the ex-situ synthesis products with 3:1 DMF:etOH ratio at times 6, 12, 24 h. The table to the right shows the determined BET surface areas.

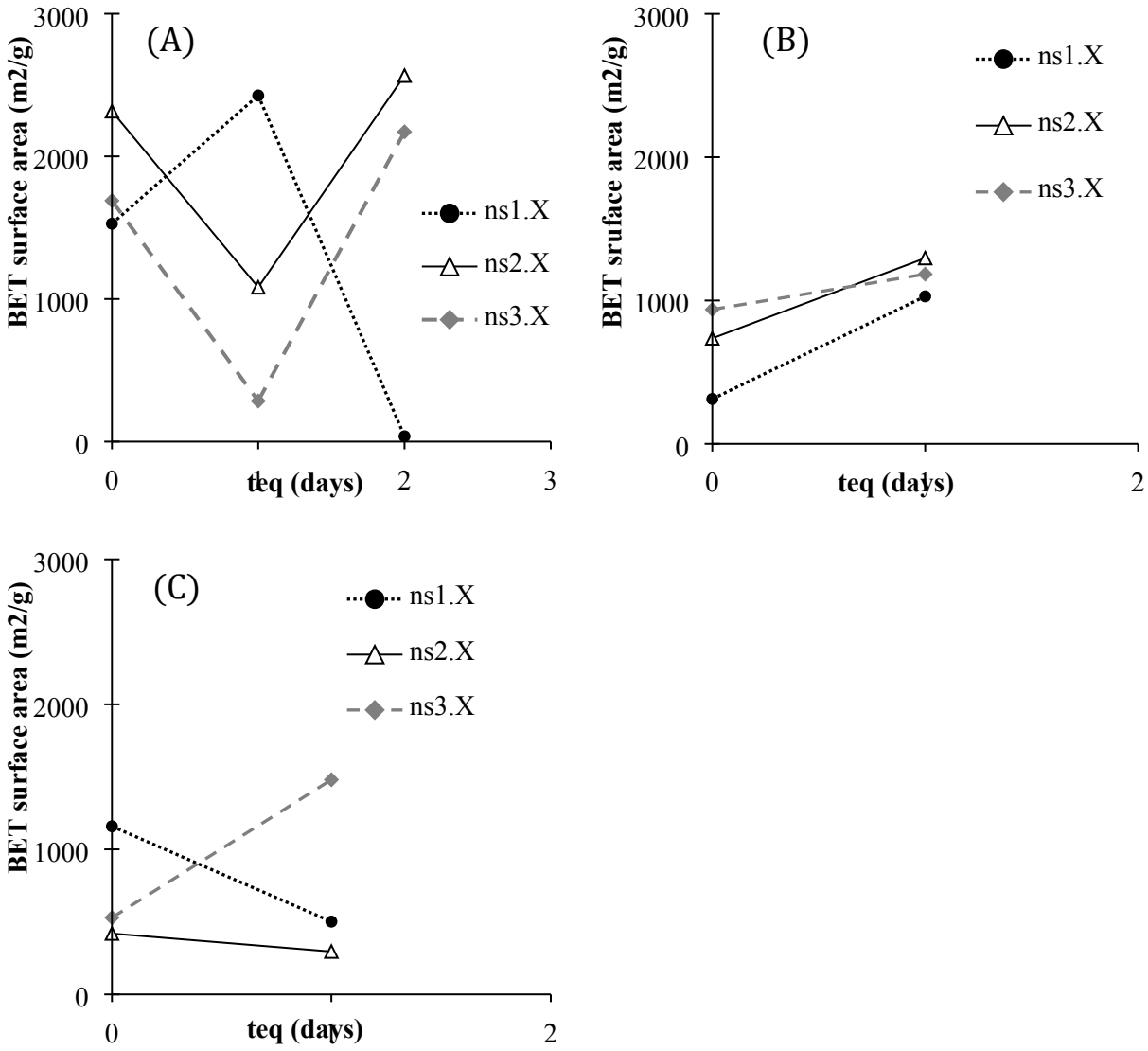

Figure 11: BET surface areas plotted against equilibration time for the syntheses with (A) 1:1 DMF:ethanol, (B) 2:1 DMF:ethanol, (C) 3:1 DMF:ethanol solvent compositions.

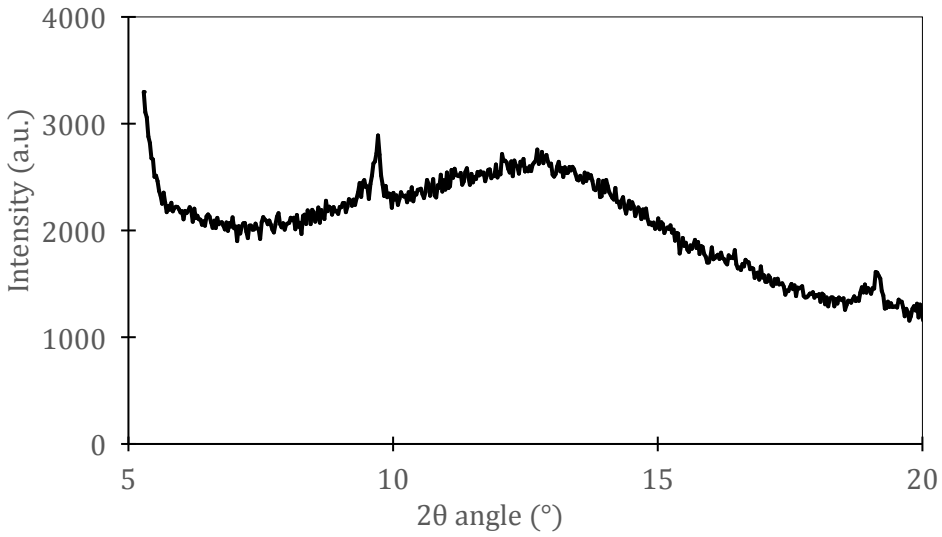

Figure S12: P-XRD (Cu Kα radiation source) pattern of ns3.1 (same as original synthesis procedure) displaying extensive fluorescence originating from iron in the sample.

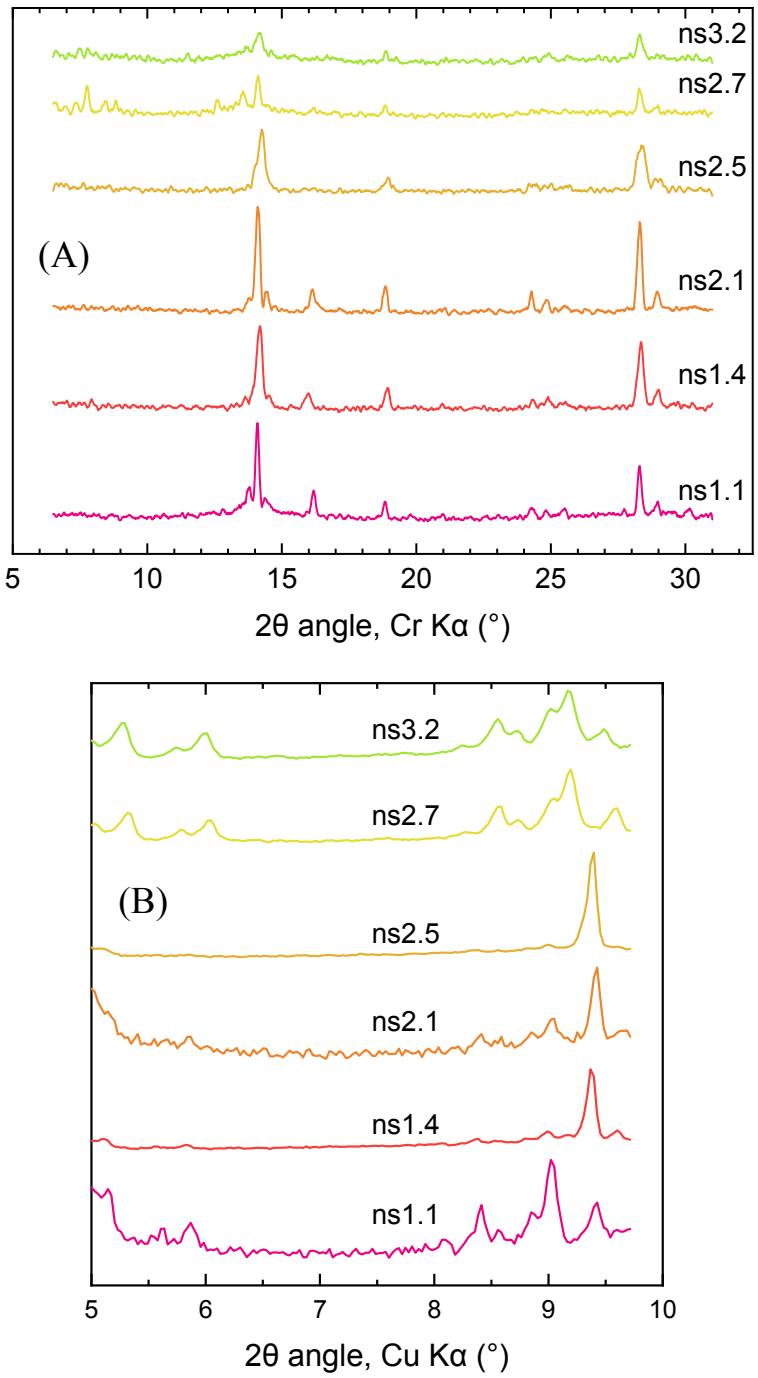

Figure S13: P-XRD diffractograms using (A) Cr Kα and (B) Cu Kα radiation. Note that due to different wavelengths of the X-rays, the 2θ angle values differ between the plots. The 2θ ranges are also different.

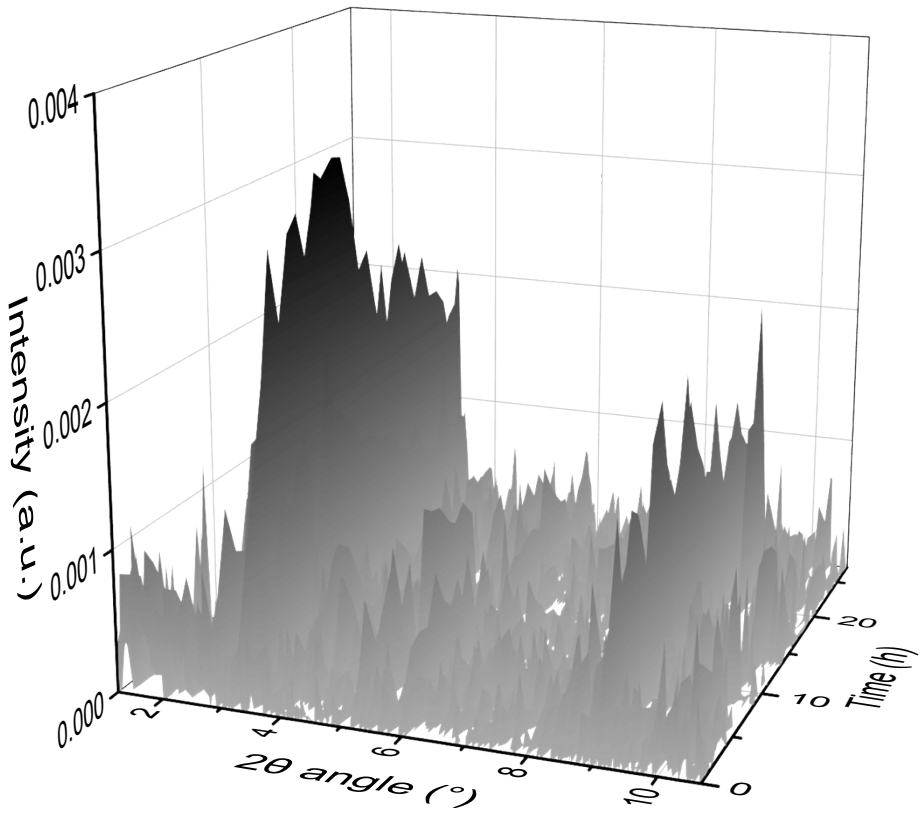

Figure S14: Time-resolved in-situ MAXS measurements of the solvothermal synthesis at 85°C using a 1:1 DMF:ethanol ratio and a 4:3 Fe(III):TPA ratio.

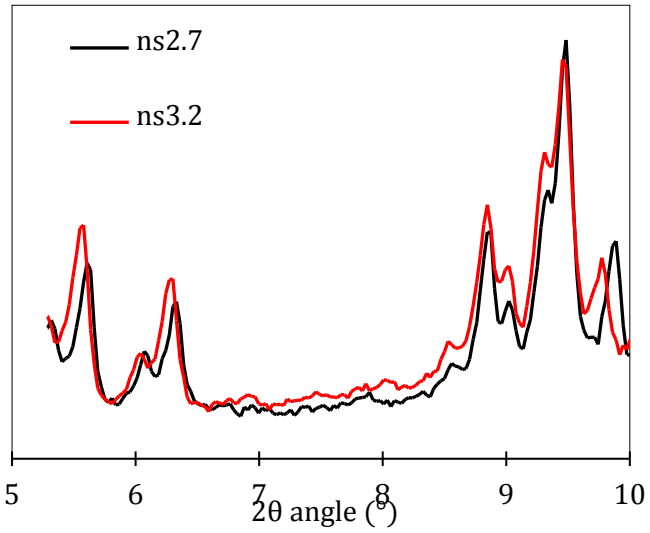

Figure S15: Comparison between the P-XRD patterns of ns2.7 and ns3.2 synthesis products. Their XRD patterns are similar but their BET surface areas differ: 2570 vs. 1690 m^2/g.

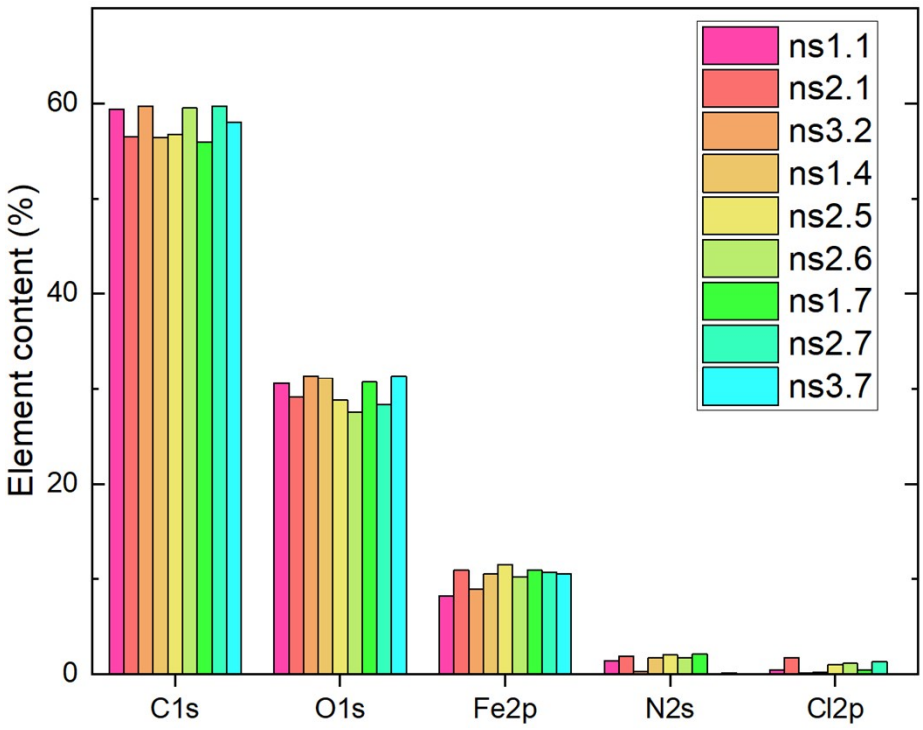

Figure S16: Element content of some of the synthesis products, obtained from XPS measurements.

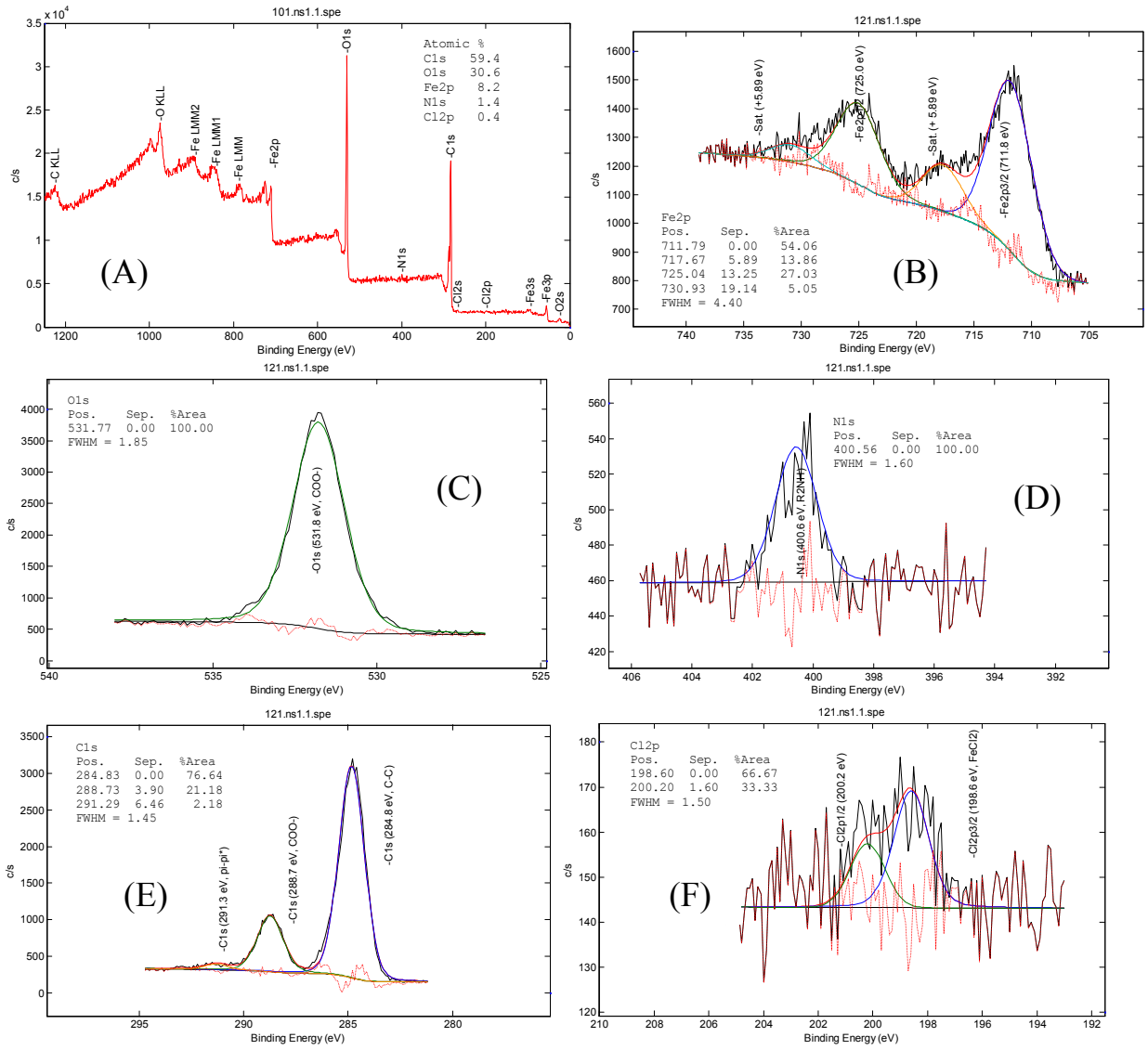

Figure S17: XPS binding energies (A) and core level spectra of (B) Fe2p, (C) O1s, (D) N1s, (E) C1s and (F) Cl2p of the ns1.1 sample (mostly MIL-101).

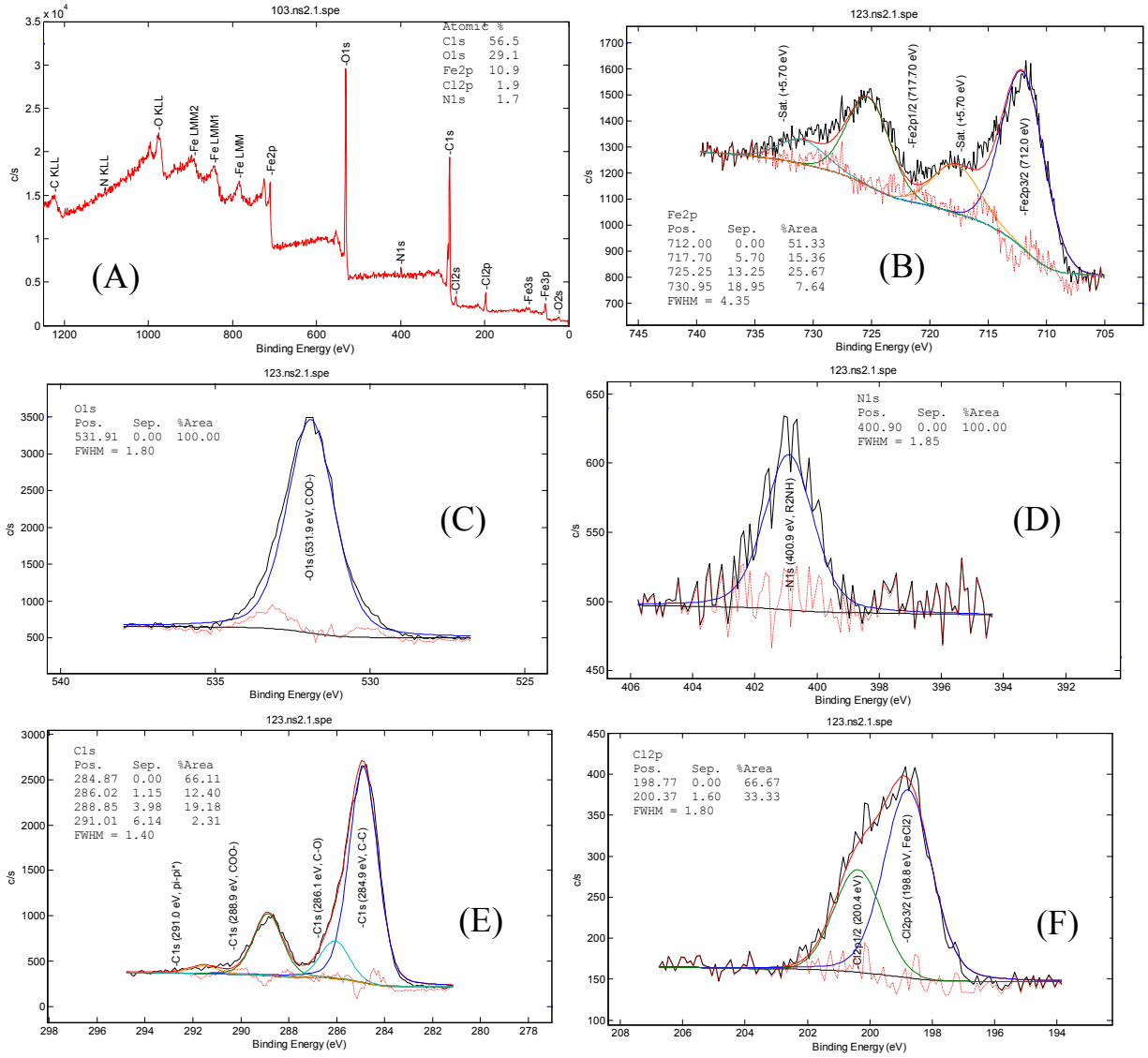

Figure S18: XPS binding energies (A) and core level spectra of (B) Fe2p, (C) O1s, (D) N1s, (E) C1s and (F) Cl2p of the ns2.1 sample (mostly MOF-235).

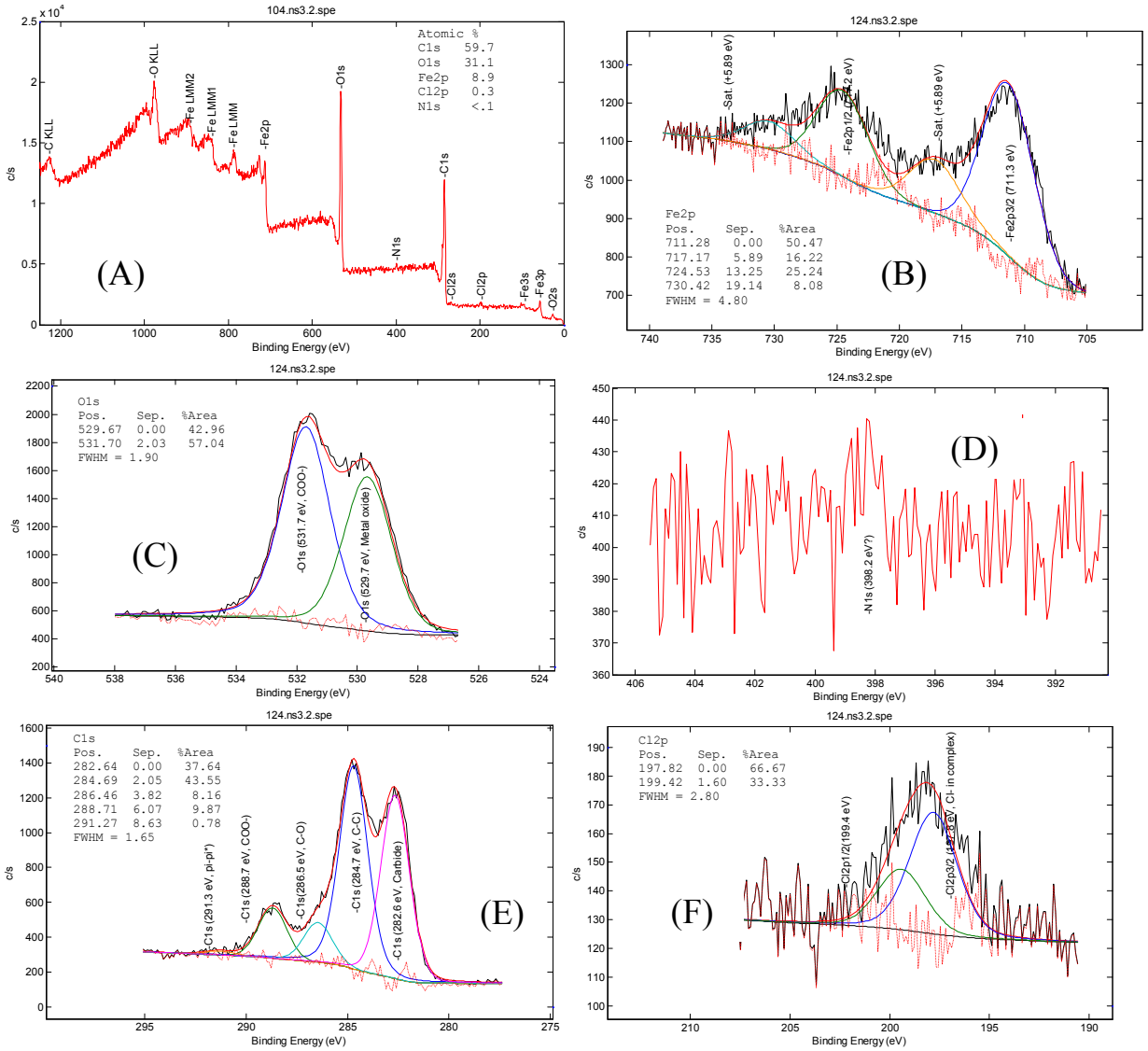

Figure S19: XPS binding energies (A) and core level spectra of (B) Fe2p, (C) O1s, (D) N1s, (E) C1s and (F) Cl2p of the ns3.2 sample (mostly MIL-101).

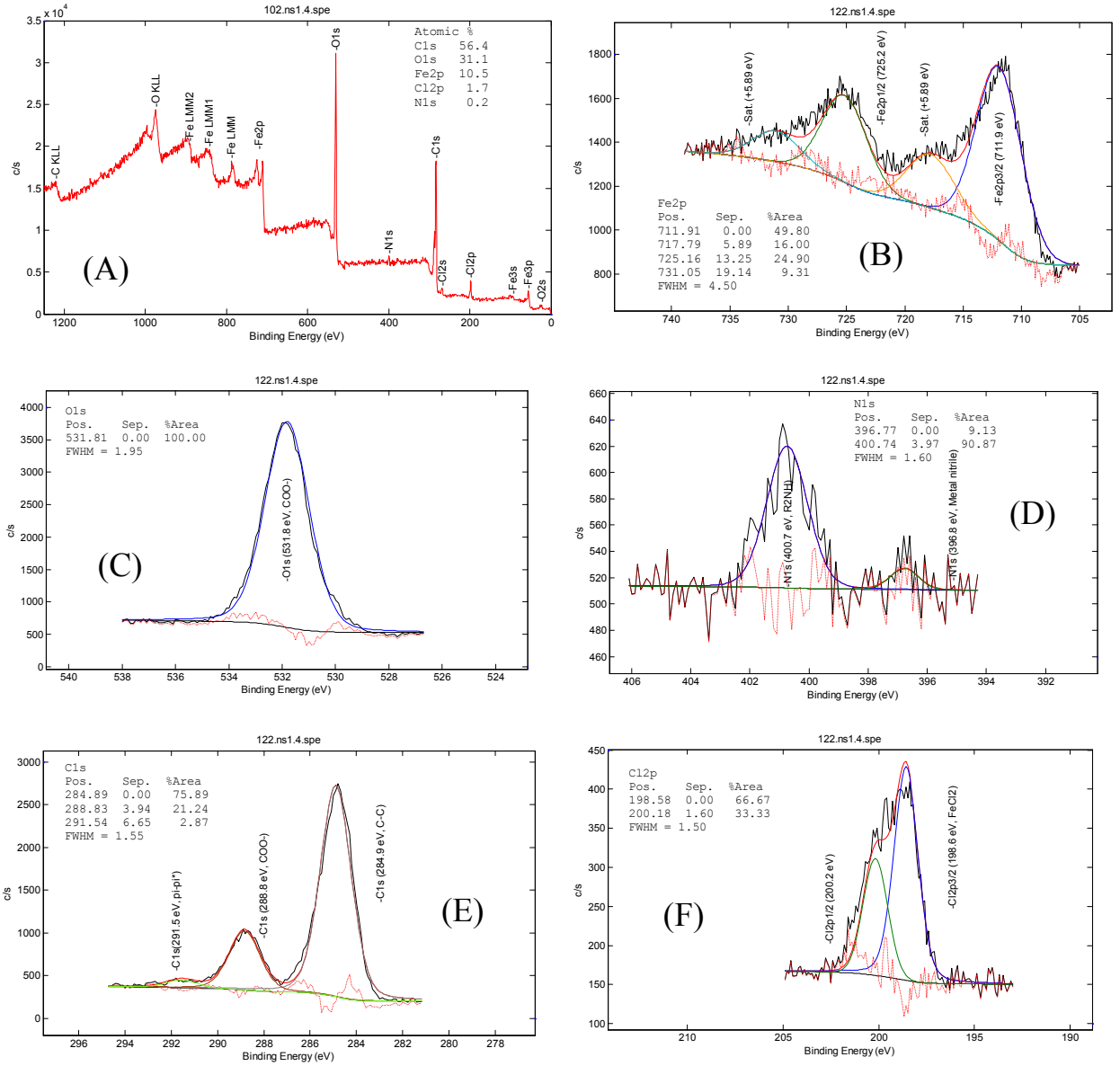

Figure S20: XPS binding energies (A) and core level spectra of (B) Fe2p, (C) O1s, (D) N1s, (E) C1s and (F) Cl2p of the ns1.4 sample (MOF-235).

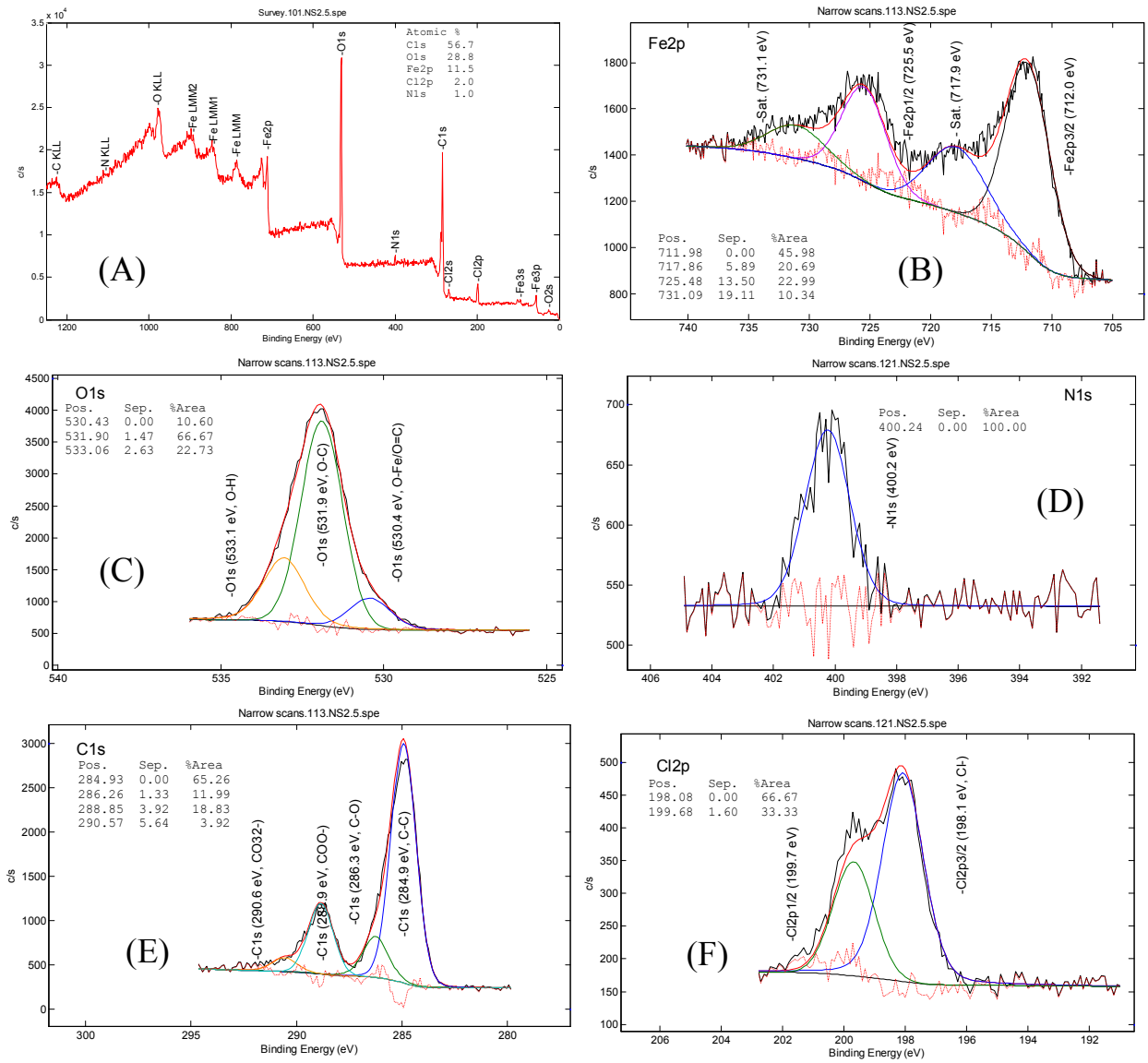

Figure S21: XPS binding energies (A) and core level spectra of (B) Fe2p, (C) O1s, (D) N1s, (E) C1s and (F) Cl2p of the ns2.5 sample (MOF-235).

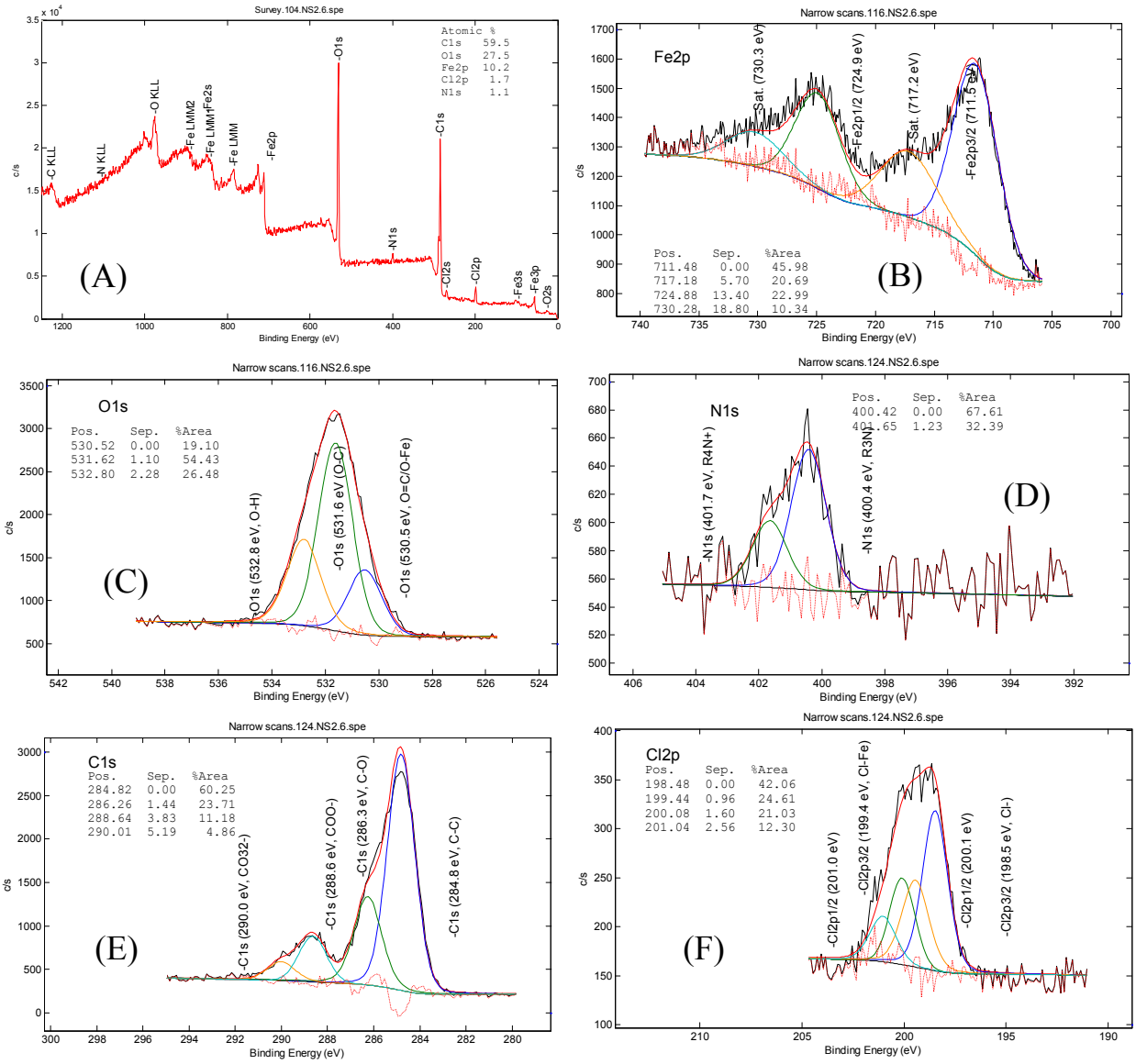

Figure S22: XPS binding energies (A) and core level spectra of (B) Fe2p, (C) O1s, (D) N1s, (E) C1s and (F) Cl2p of the ns2.6 sample (MOF-235).

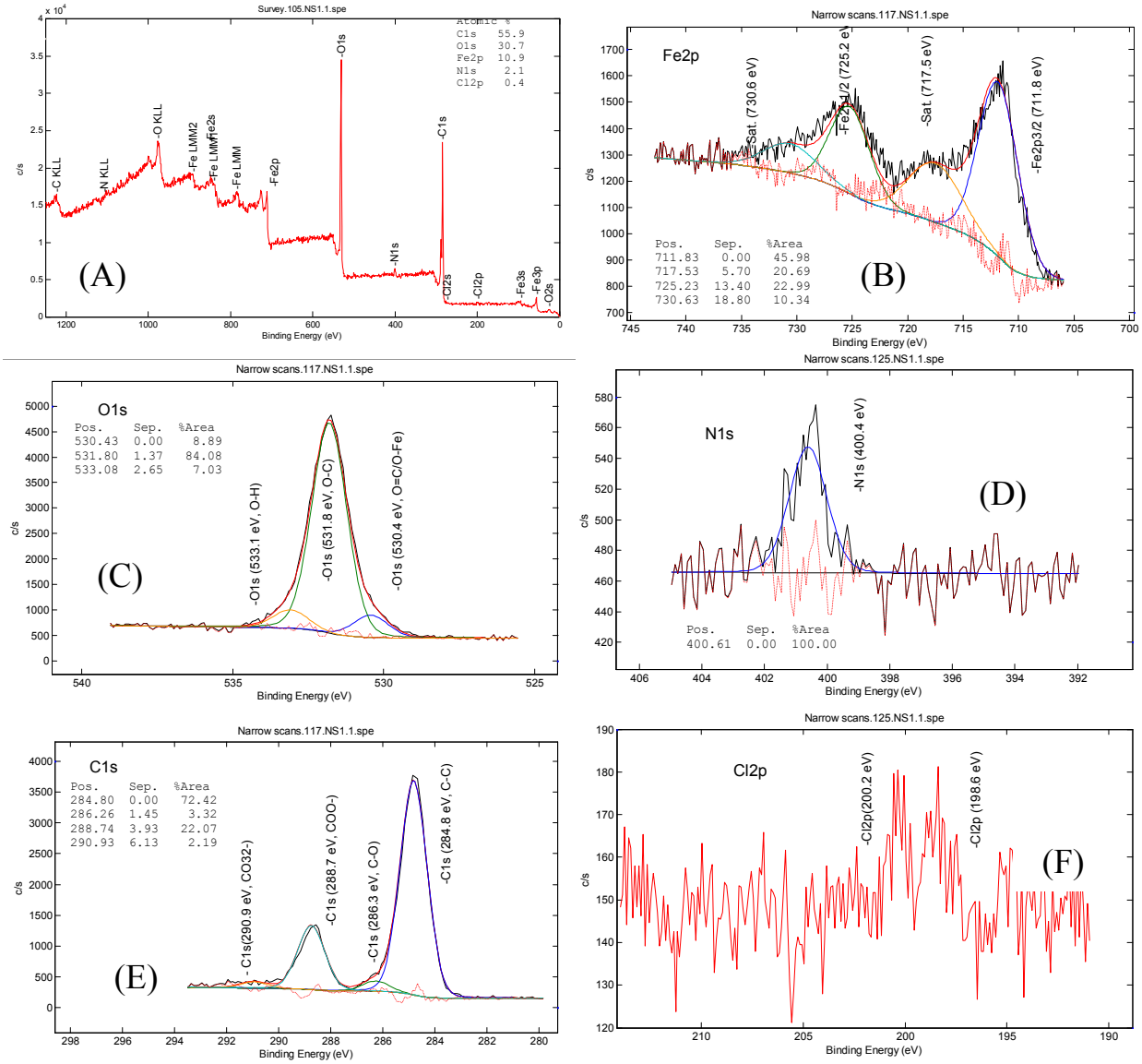

Figure S23: XPS binding energies (A) and core level spectra of (B) Fe2p, (C) O1s, (D) N1s, (E) C1s and (F) Cl2p of the ns1.7 sample (slightly amorphous MOF-235).

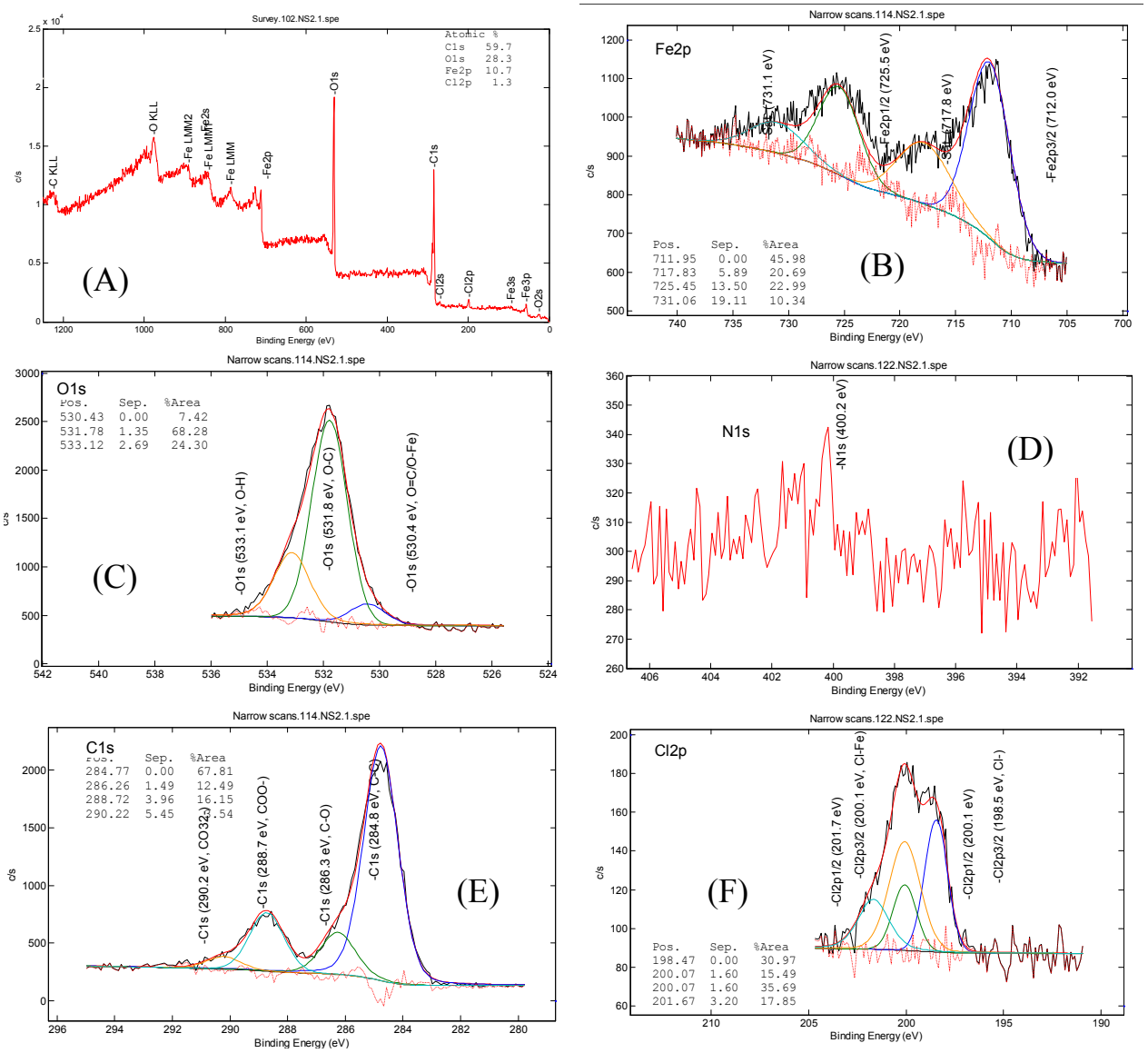

Figure S24: XPS binding energies (A) and core level spectra of (B) Fe2p, (C) O1s, (D) N1s, (E) C1s and (F) Cl2p of the ns1.7 sample (slightly amorphous MOF-235).

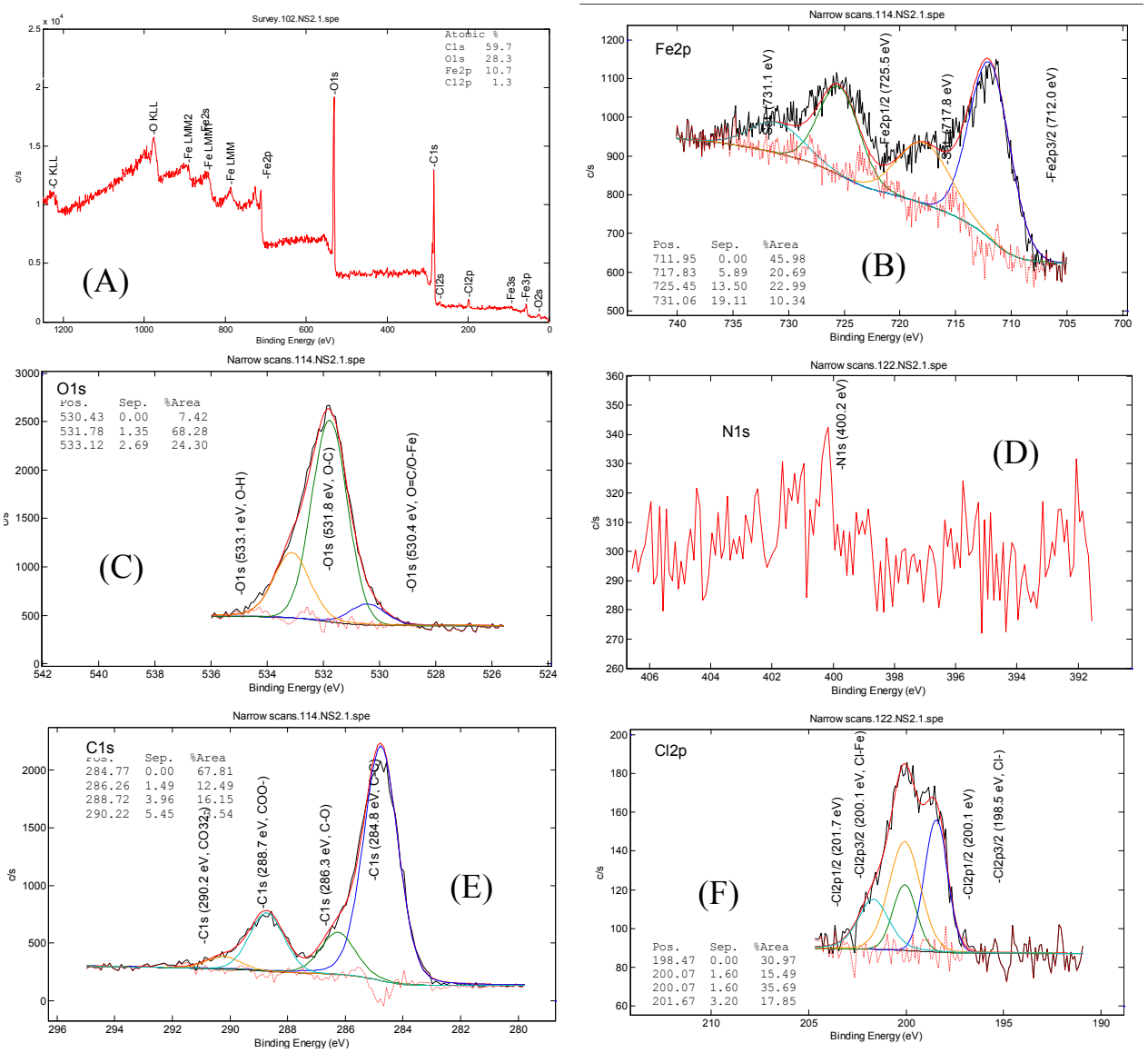

Figure S25: XPS binding energies (A) and core level spectra of (B) Fe2p, (C) O1s, (D) N1s, (E) C1s and (F) Cl2p of the ns1.7 sample (slightly amorphous MOF-235).

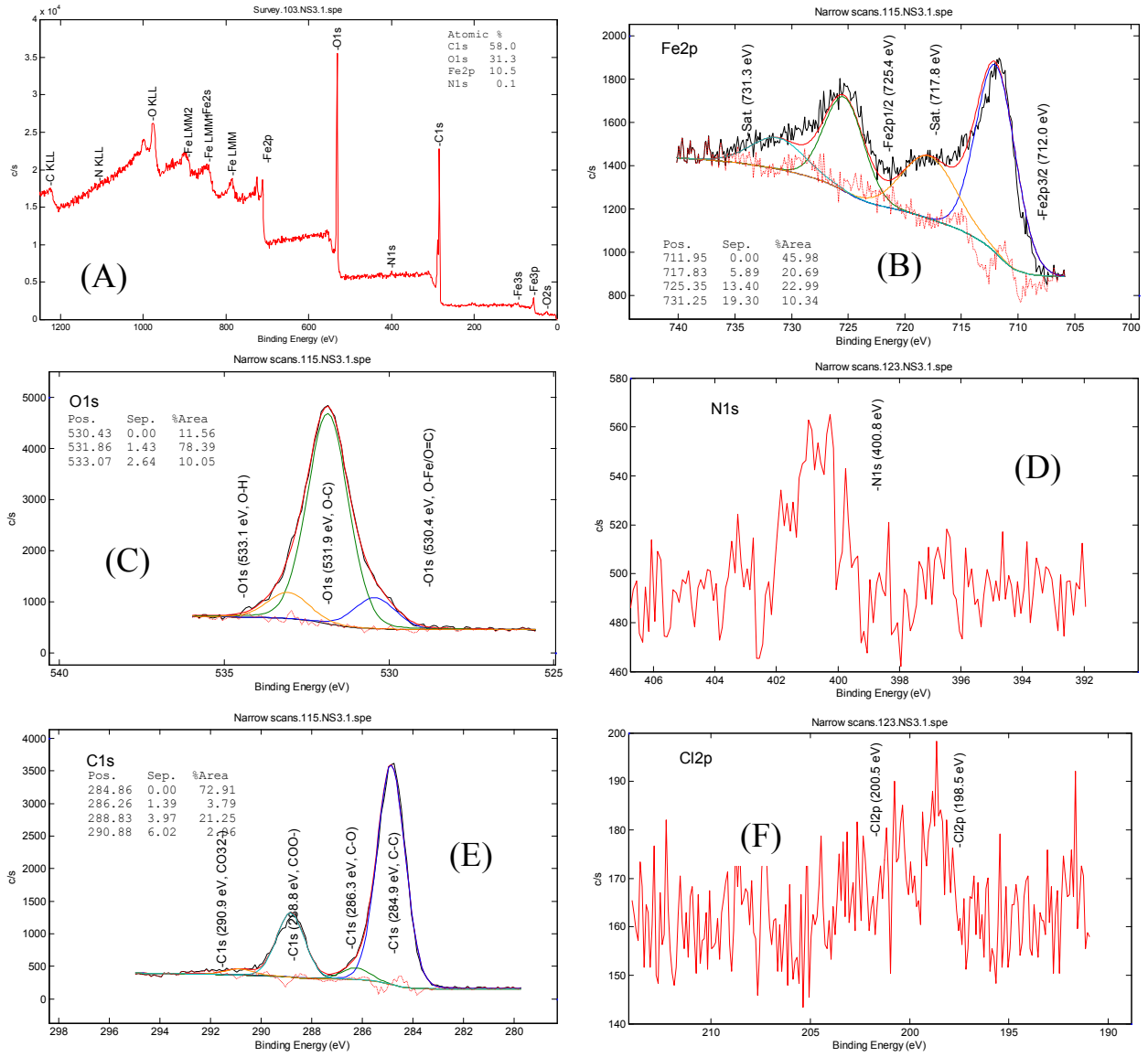

Figure S26: XPS binding energies (A) and core level spectra of (B) Fe2p, (C) O1s, (D) N1s, (E) C1s and (F) Cl2p of the ns1.7 sample (partially amorphous MOF-235).

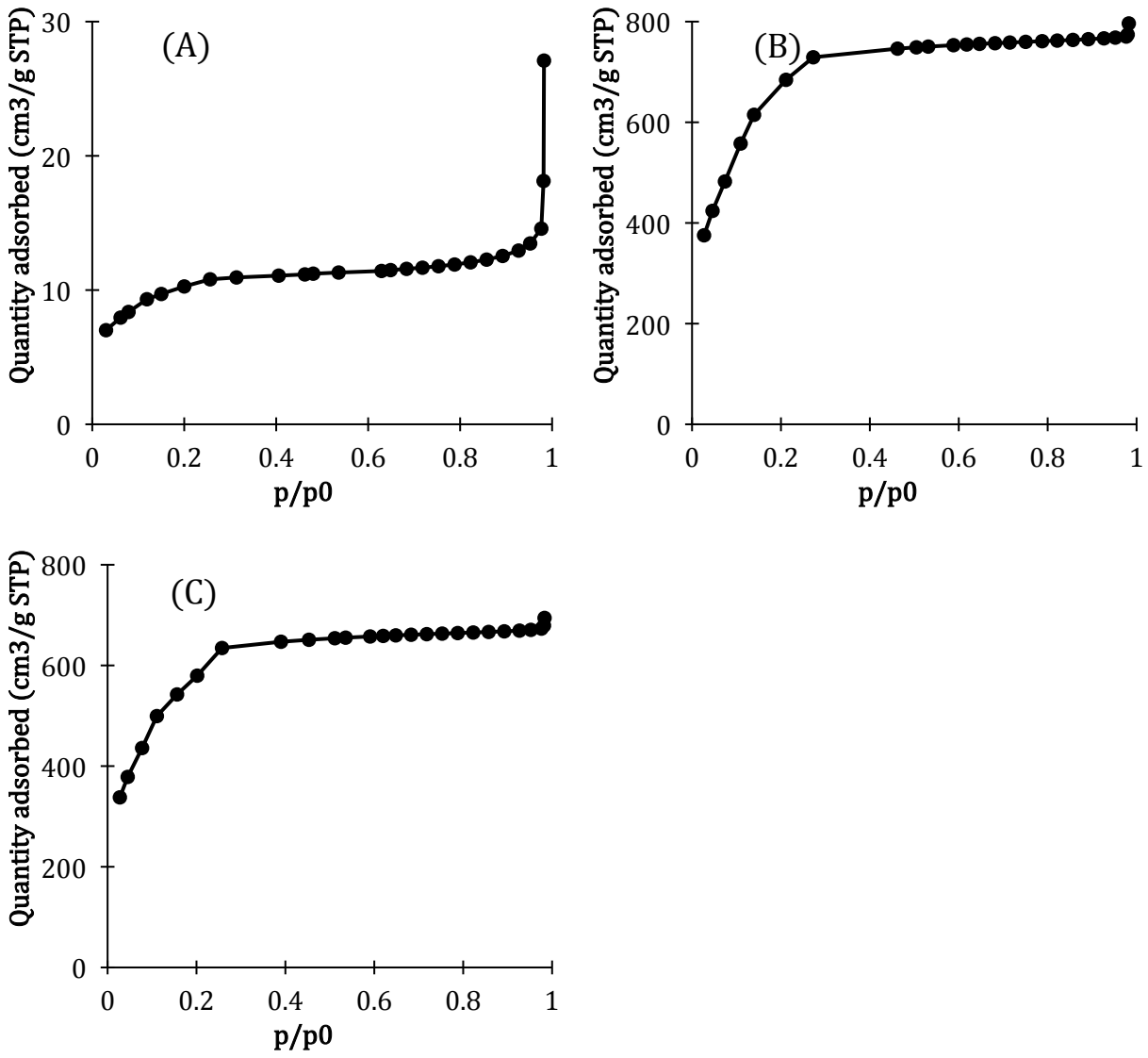

Figure S27: Nitrogen adsorption isotherms of the (A) ns1.7, (B) ns2.7, (C) ns3.7 synthesis products used to determine the respective BET surface areas.

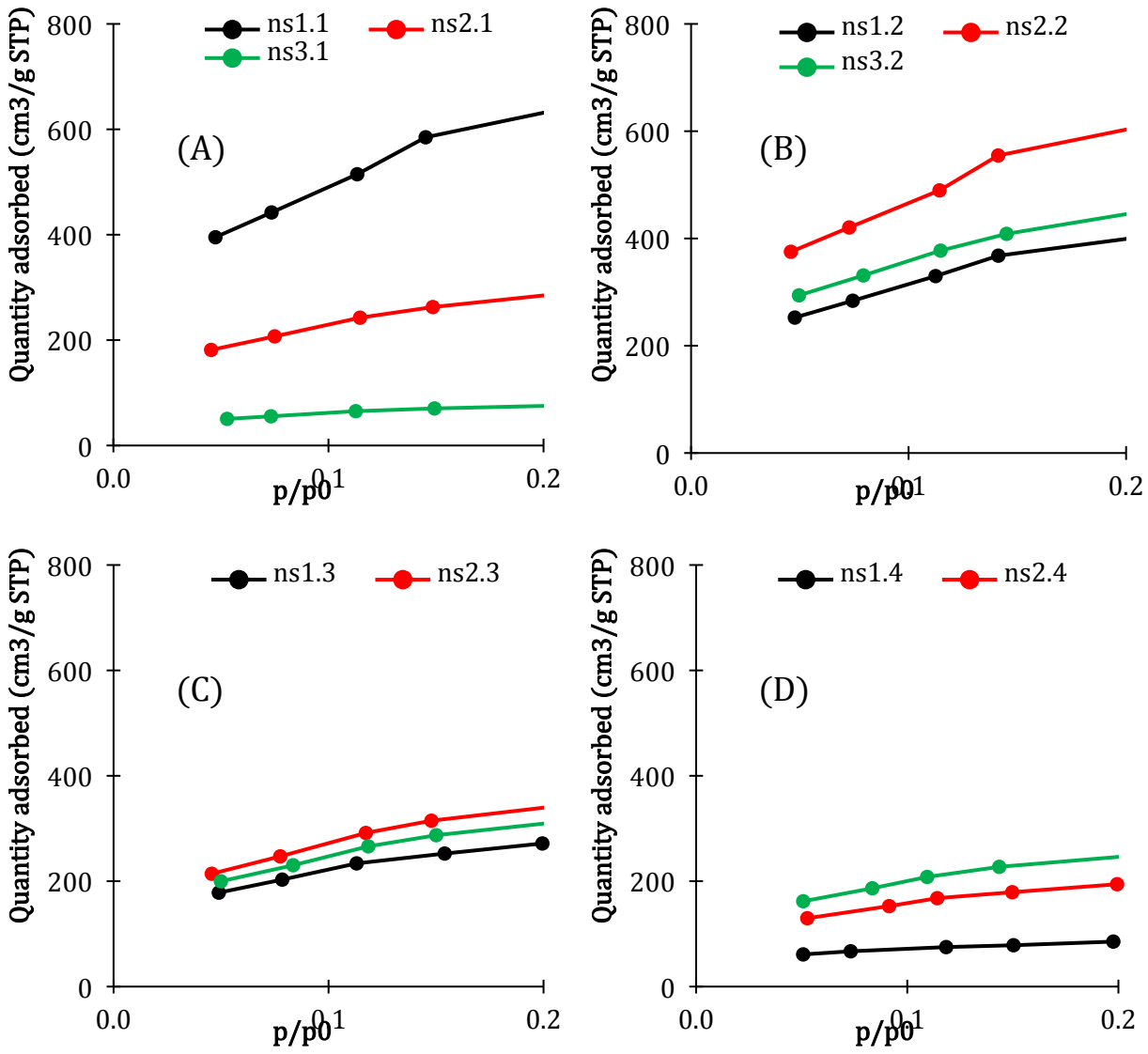

Figure S28: Nitrogen adsorption isotherms of the (A) nsX.1, (B) nsX.2, (C) nsX.3, (D) nsX.4 synthesis products used to determine the respective BET surface areas.

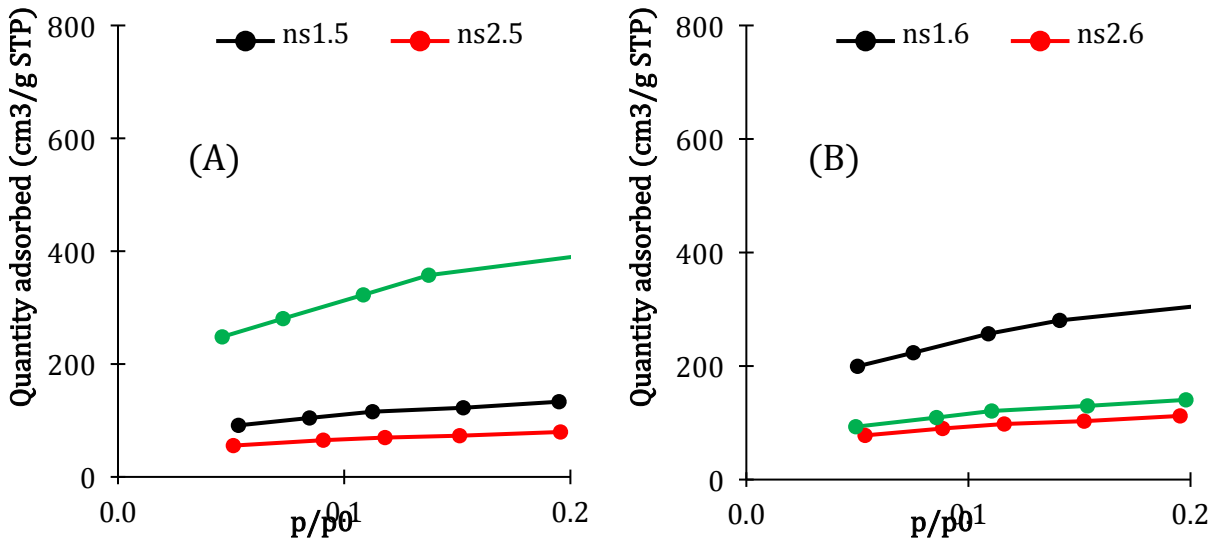

Figure S29: Nitrogen adsorption isotherms of the (A) nsX.5, (B) nsX.6 synthesis products used to determine the respective BET surface areas.

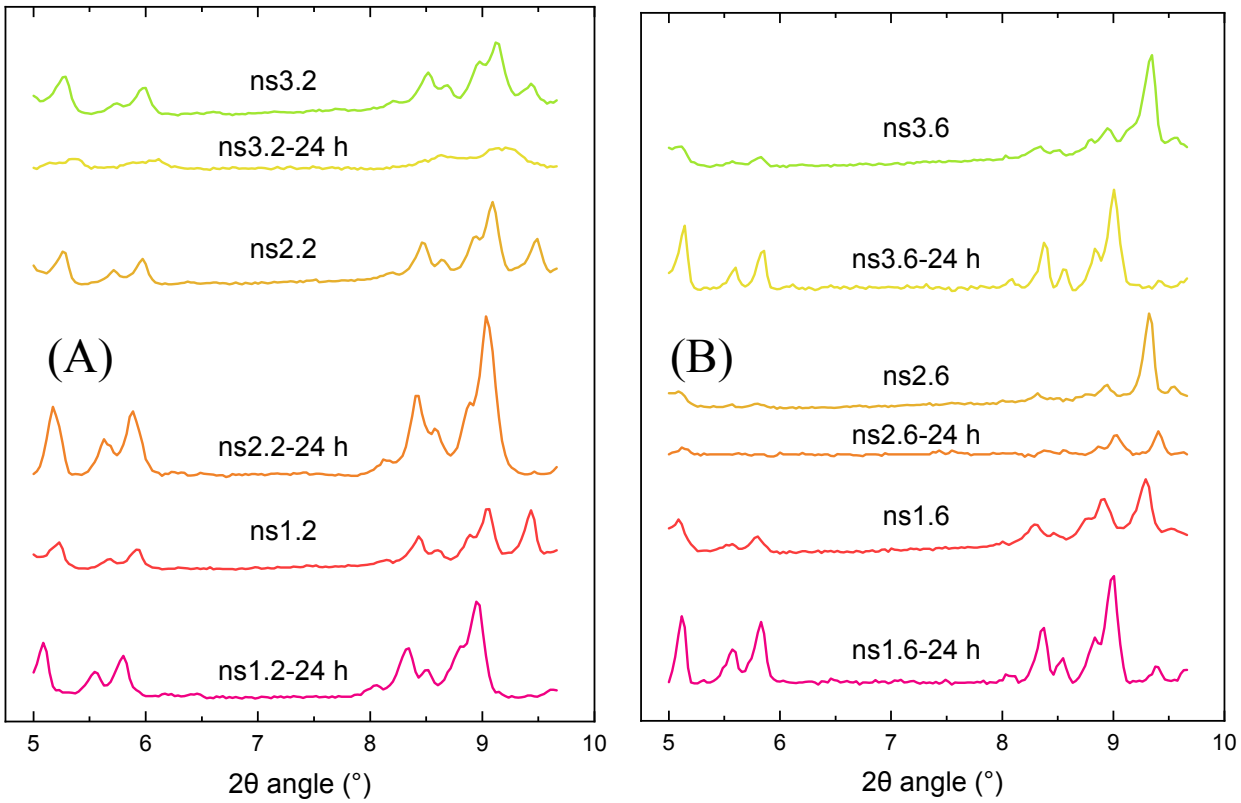

Figure S30: Comparison between XRD patterns of 24 h ex-situ products ("nsX.X-24 h") and regular solvothermal products treated for 24 h at 80°C ("nsX.X"). The syntheses were either conducted with a (A) 1:1 or (B) 3:1 DMF:etOH solvent ratio.

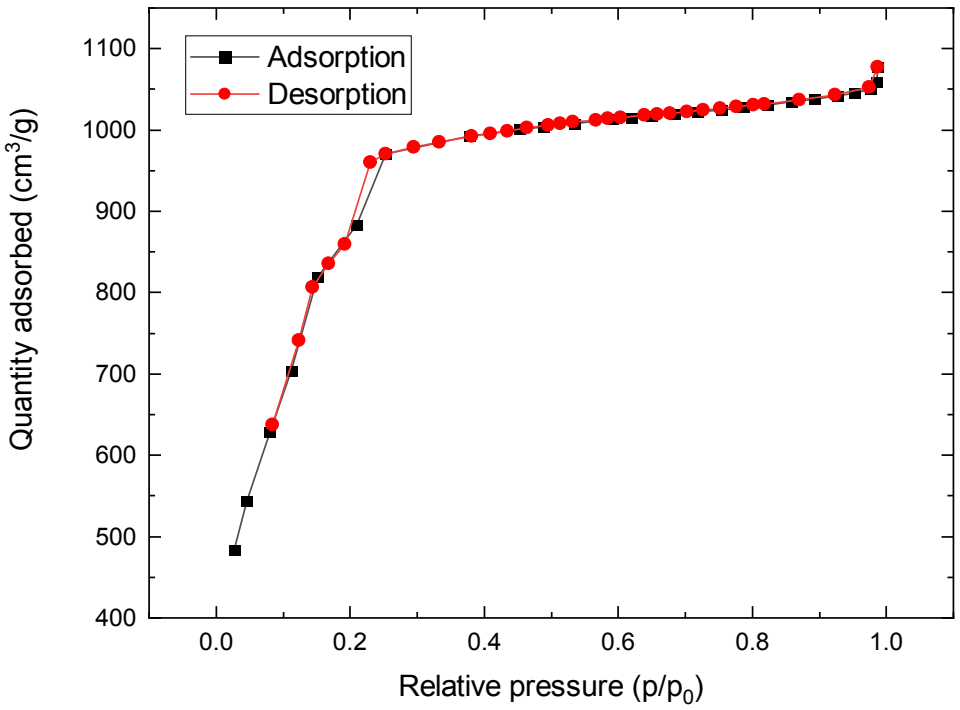

Figure S31: Full N_2 adsorption and desorption isotherms of the largest surface area product from the "ex-situ synthesis" (ns2.2-24 h, XRD shown in Figure S9).

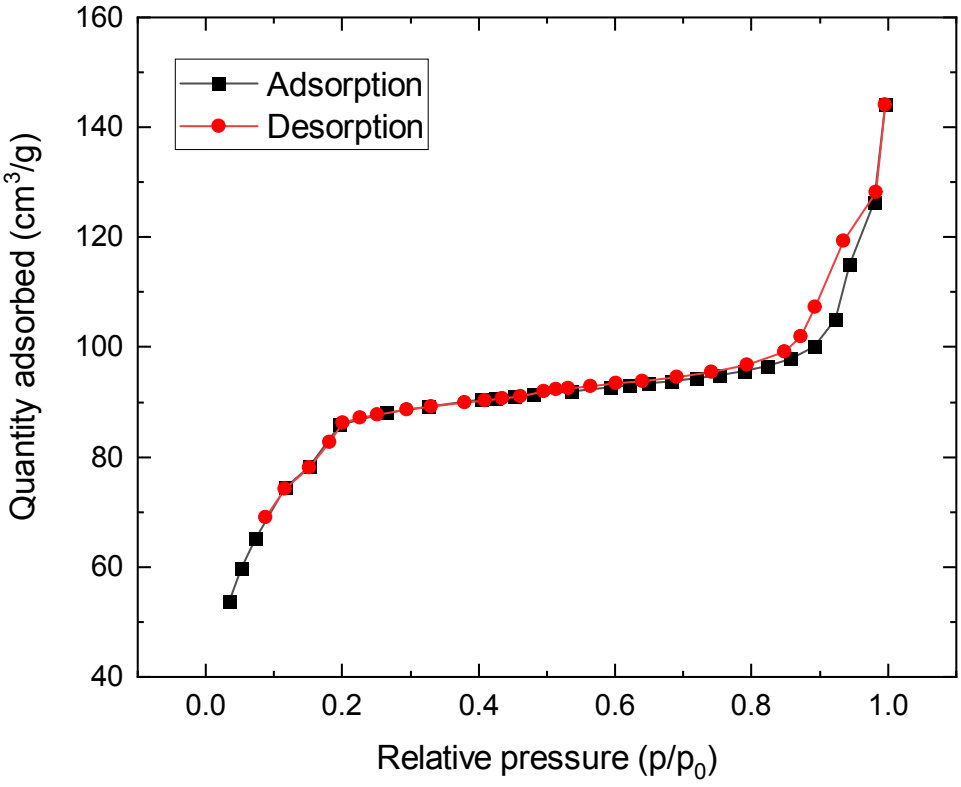

Figure S32: Full N_2 adsorption and desorption isotherms of ns2.6 (MOF-235(Fe)).

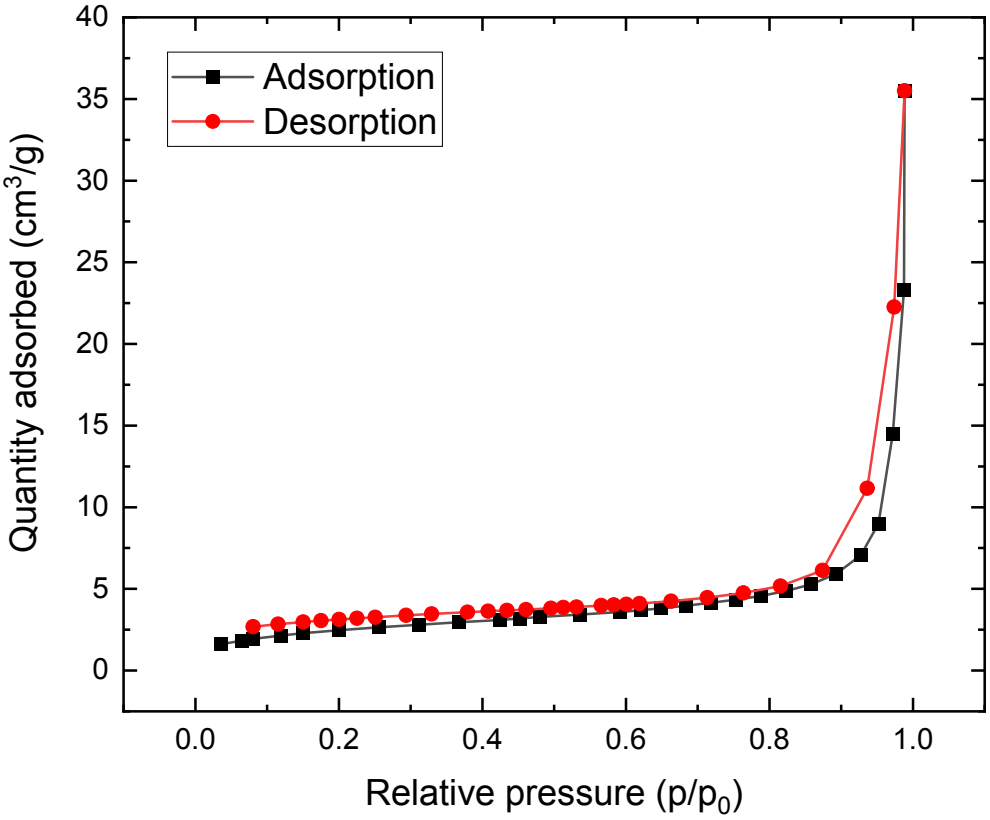

Figure S33: Full N_2 adsorption and desorption isotherms of ns2.5 (MOF-235(Fe)) after 1 year of storage in desiccator.

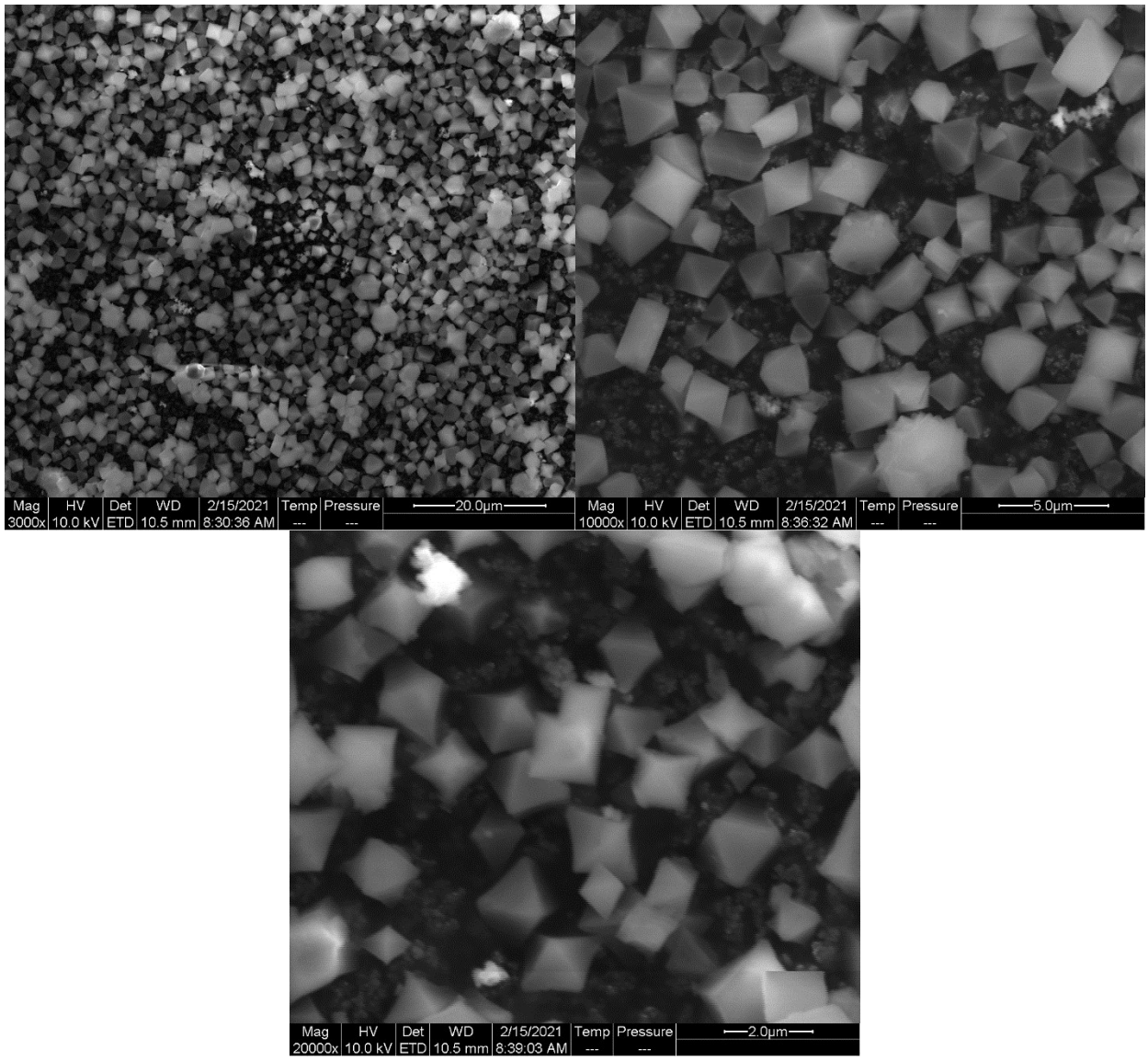

Figure S34: SEM images of ns2.2-24 h (MIL-101(Fe)) at different magnification levels. Synthesis date: September 2020.

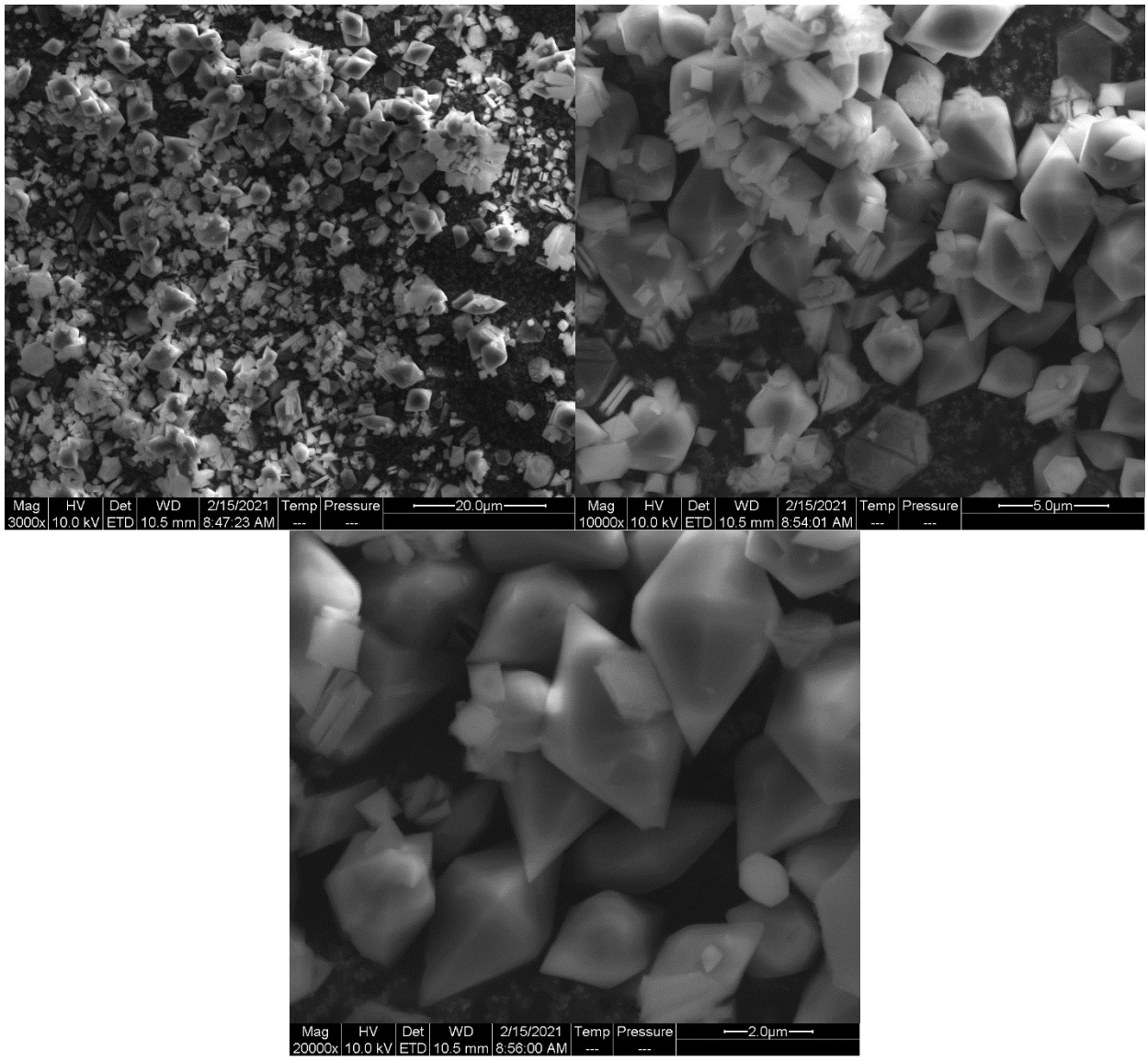

Figure S35: SEM images of ns2.5 (MOF-235(Fe)) at different magnification levels. Synthesis date: January 2020.

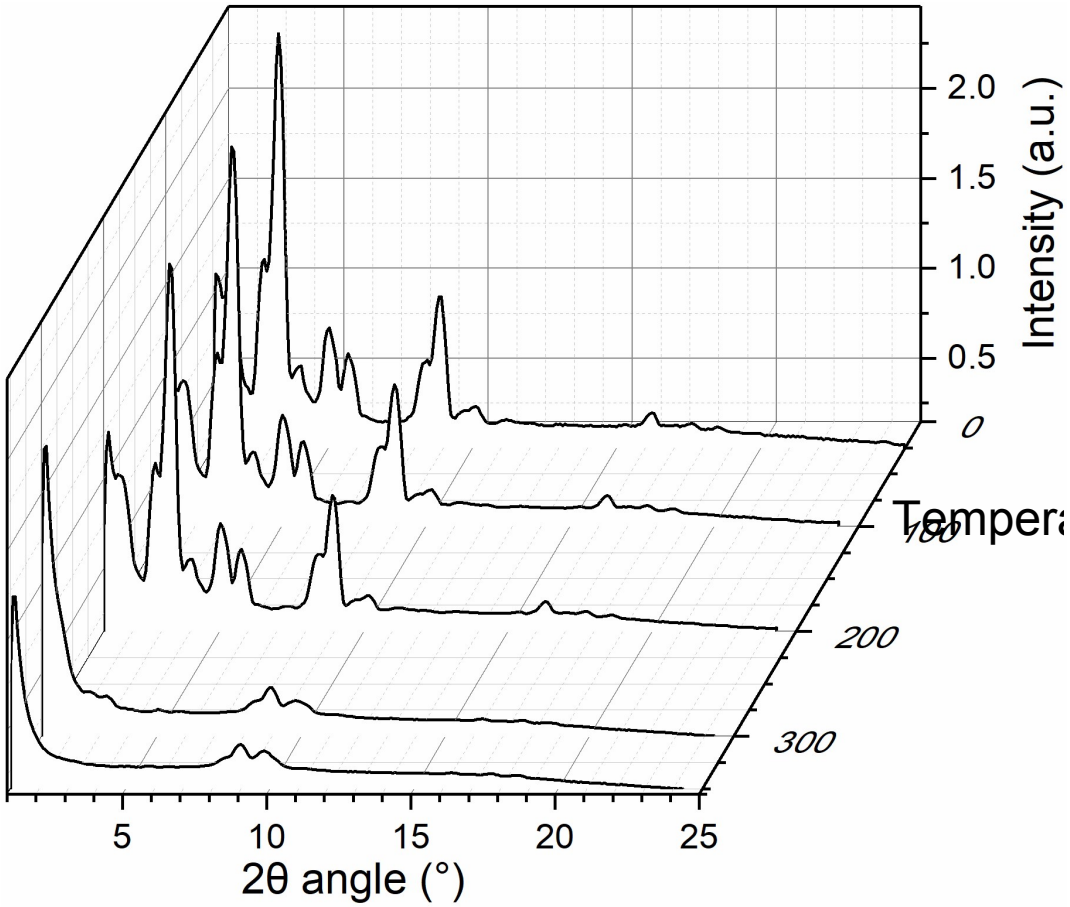

Figure S36: XRD diffractograms at T = 25, 100, 200, 300, 350°C of ns2.2-24 h (MIL-101(Fe)).

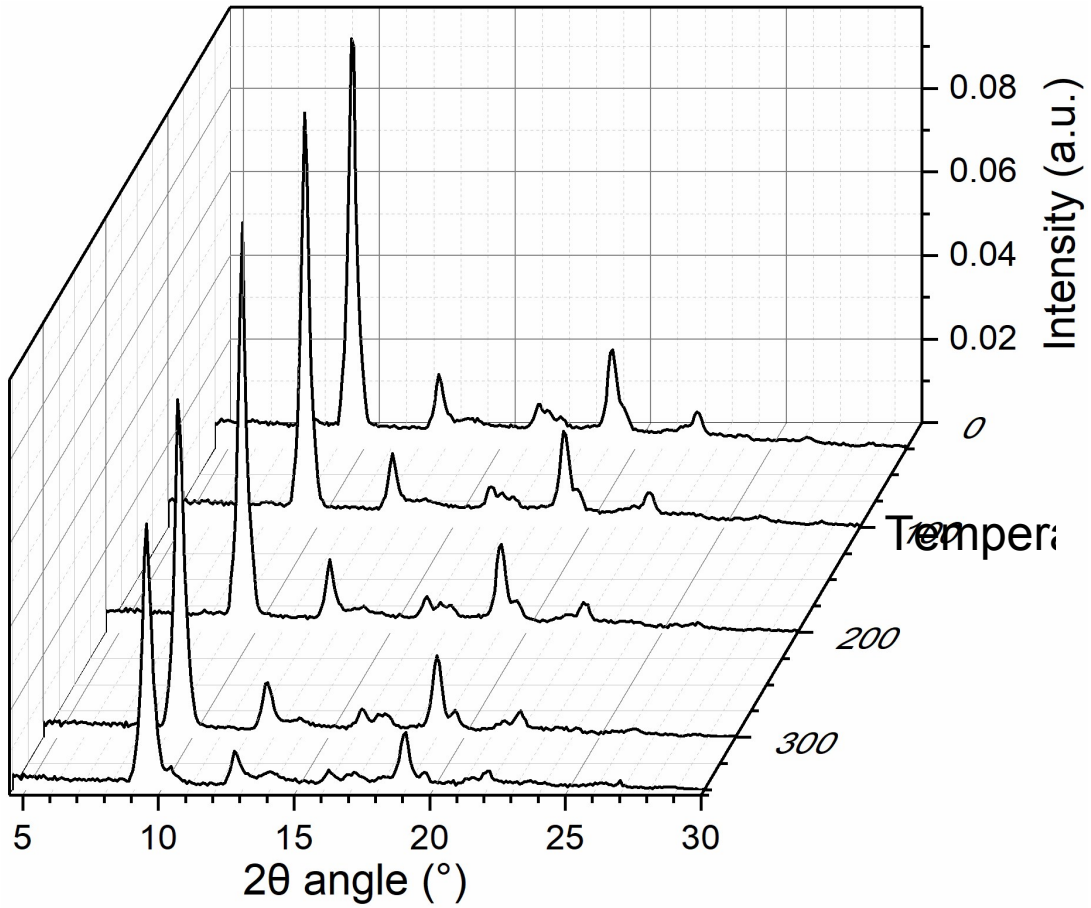

Figure S37: XRD diffractograms at T = 25, 100, 200, 300, 350°C of ns2.5 (MOF-235(Fe)).

Tables.

Table S1: Elemental analysis by XPS of some of the synthesized solid products.

Synthesis	C content (%)	N content (%)	O content (%)	Cl content (%)	Fe content (%)
ns2.5	56.7	1.0	28.8	2.0	11.5
ns2.1	59.7	0	28.3	1.0	10.7
ns3.1	58.0	0.1	31.3	0	10.5
ns2.6	59.5	1.1	27.5	2.0	10.2
ns1.1	55.9	2.1	30.7	0	10.9

Table S2: pH measurements of dispersions of ns2.1 (MIL-101) and ns2.7 (MOF-235) before and after methylene blue adsorption.

Synthesis product	Sample #	pH_0	pH_{after}
ns2.1	1	3.91	4.32
	2	3.80	4.69
	3	3.79	4.70
	Average	3.83	4.57
ns2.7	1	3.99	4.98
	2	3.86	4.68
	3	3.94	4.87
	Average	3.93	4.84

Bibliography

1. K. B. H. Putz, *Journal*.
2. O. Lebedev, F. Millange, C. Serre, G. Van Tendeloo and G. Férey, *Chemistry of materials*, 2005, **17**, 6525-6527.
3. A. C. Sudik, A. P. Côté and O. M. Yaghi, *Inorganic chemistry*, 2005, **44**, 2998-3000.